NOTICE

The quality of this microfiche is heavily dependent upon the quality of the original thesis submitted for microfilming. Every effort has been made to ensure the highest quality of reproduction possible.

If pages are missing, contact the university which granted the degree.

Some pages may have indistinct print especially if the original pages were typed with a poor typewriter ribbon or if the university sent us a poor photocopy.

Previously copyrighted materials (journal articles, published tests, etc.) are not filmed.

Reproduction in full or in part of this film is governed by the Canadian Copyright Act, R.S.C. 1970, c. C-30. Please read the authorization forms which accompany this thesis.

THIS DISSERTATION
HAS BEEN MICROFILMED
EXACTLY AS RECEIVED

AVIS

La qualité de cette microfiche dépend grandement de la qualité de la thèse soumise au microfilmage. Nous avons tout fait pour assurer une qualité supérieure de reproduction.

S'il manque des pages, veuillez communiquer avec l'université qui a conféré le grade.

La qualité d'impression de certaines pages peut laisser à désirer, surtout si les pages originales ont été dactylographiées à l'aide d'un ruban usé ou si l'université nous a fait parvenir une photocopie de mauvaise qualité.

Les documents qui font déjà l'objet d'un droit d'auteur (articles de revue, examens publiés, etc.) ne sont pas microfilmés.

La reproduction, même partielle, de ce microfilm est soumise à la Loi canadienne sur le droit d'auteur, SRC 1970, c. C-30. Veuillez prendre connaissance des formules d'autorisation qui accompagnent cette thèse.

LA THÈSE A ÉTÉ
MICROFILMÉE TELLE QUE
NOUS L'AVONS REÇUE

PROPERTIES OF QUATERNARY III-V SEMICONDUCTING ALLOYS

by

Kim Zbitnew

A Thesis
presented to the University of Ottawa
in partial fulfillment of the
requirements for the degree of
MSc.
in
Physics

Ottawa, Ontario, 1980

UNIVERSITÉ D'OTTAWA
UNIVERSITY OF OTTAWA

ABSTRACT

Ingots of $Al_xGa_yIn_{1-x-y}Sb$ were grown using a directional freezing technique. Slices were taken from these ingots, and their compositions were determined by an X-ray fluorescence method. X-ray powder photographs were taken of the slices, and if they were single phase, the lattice parameters and minimum energy gaps were determined. The energy gaps were determined by simple transmission. Empirical equations were derived from the data to fit the lattice parameter and energy gaps as a function of composition.

TABLE OF CONTENTS

ABSTRACT ii

Chapter page

I. INTRODUCTION 1

II. GROWTH OF THE ALLOYS 4

Introduction 4
Preparing single phase material 5
Directional freezing 7
Furnaces 8
Theory of directional freezing 10
Problems of directional freezing 11
Obtaining slices 12

III. DETERMINATION OF COMPOSITION 14

Introduction 14
Theory of XRF 14
Instrumentation 16
Using the counts 19
Sample preparation and sample holders 23
Sample holders 27
The Lachance equation 28
Terminology 30
Determination of the α coefficients 32
Graphical analysis of the data 34
Comparison of theory with experimental data . . 37
Composition determination 38
Reliability of the composition determination . 39
Composition of the unknown ingots 40
Evidence of reliability of the composition data 41

IV. DETERMINATION OF THE LATTICE PARAMETER 54

Further evidence of the reliability of the composition data 55

V. ENERGY GAP DETERMINATION 62

VI. FITTING THE DATA 72

Introduction 72

Fitting the lattice parameter data 72
Fitting the Eg data 73
Direct gap 74
Indirect gap 76
Summary 76
Notes about the fits 77

VII. THERMODYNAMIC DATA 81

VIII. CONCLUSIONS 83

References 84

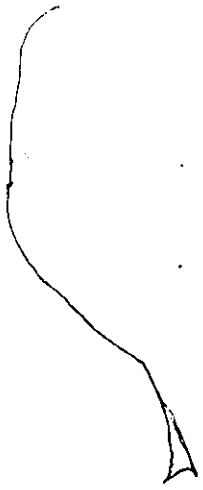

LIST OF TABLES

Table page

1. Summary of the XRF measurements 22
2. The α coefficients and the C100's 36
3. Comparison of compositions determined from the α coefficients with the actual compositions 37
4. Count ratios as a function of composition 39
5. Ratios of Theoretical/actual starting compositions of the ingots 42
6. Comparison of compositions determined from lattice parameters with those determined from XRF 56
7. Comparison of compositions determined from absorption measurements with those determined by XRF 66
8. Summary of data and sources used in fitting the energy gap data 75

LIST OF FIGURES

Figure		page
1.	A typical binary phase diagram	6
2.	Simplified diagram of an X-ray spectrometer	15
3.	Sample holders	28
4.	Triangular coordinates	43
5.	Apparatus used in the transmission measurements	63
6.	Some typical absorption curves	65

LIST OF GRAPHS

Graph		page
1	Composition vs distance for Ingot DF AGIS 103060#2	44
2	" " " " 104545#2	45
3	" " " 161668	46
4	" " " 201070	47
5	" " " 252550	48
6	Composition(triangular coordinates) of Ingot DF AGIS 103060#2	49
7	" " " 104545#2	50
8	" " " 161668	51
9	" " " 201070	52
10	" " " 252550	53
11	Lattice parameter vs distance for Ingot DF AGIS 103060#2	57
12	" " " 104545#2	58
13	" " " 161668	59
14	" " " 201070	60
15	" " " 252550	61
16	Energy gap vs position for Ingot DF AGIS 103060#2	67
17	" " " 104545#2	68
18	" " " 161668	69
19	" " " 201070	70
20	" " " 252550	71
21	Lattice parameter contours	78
22	Direct gap contours	79
23	Indirect gap contours	80
24	Tie Lines	82

Acknowledgements

I would like to thank my supervisor, Dr. J.C. Woolley, for invaluable advice, and Mr. Gerald Goodchild, for assistance in the use of the optical equipment. I would also like to thank the Geology department for making the XRF equipment available, and Mr. Ron Hartree who helped me use it.

Chapter I

INTRODUCTION

The quaternary III-V semiconducting alloys studied here are chemical compounds of the form $A_xB_yC_{1-x-y}D$, where A,B, and C represent elements in group III of the periodic table and D represents an element in group V of the periodic table. In this case , A,B, and C are Al, Ga, and In respectively, and D is Sb. x and y represent atomic fractions of AlSb and GaSb respectively, in the alloy system. x and y are independent quantities, and may take any value,provided their sum does not exceed 1. In simple terms, one may suppose that the formula represents a structure that consists of one group III atom to every atom of antimony. x is just the fraction of the group III atoms that are aluminum, and so forth, and overall there is just one group III atom to every atom of antimony.

The main purpose of the present work was to find out how certain properties of the alloy system varied as x and y varied. Since x and y may be varied independently, a given property in general depends on both x and y. Thus it is possible to find a series of x and y such that a certain property is a constant. However, in general, a second property

will not be a constant for the same series of x and y. This amounts to being able to make independent selections of any two (independent) properties of a quaternary alloy system (the limits of the selection depending on the range of possible properties).

In the present work, the properties studied were primarily the lattice parameter and the minimum energy gap. It is useful to know these properties because the energy gap determines the wavelength of light obtained when the semiconductor is used for making some light emitting device, and the lattice parameter is significant in regards to the growth of thin layers of the material.

As a practical example of the utility of quaternary alloys, consider the construction of an LED (light emitting diode). The selection of a material with which to make the diode may be limited by the particular wavelength of light desired. However, if one is making the material by liquid phase epitaxy, good layers can be made only if the lattice parameter of the layer is closely matched to that of the substrate (what the layer is grown on). With a quaternary alloy, the two independent variables x and y (as mentioned earlier) allow one to select an alloy with a lattice parameter matching that of the substrate, yet also allows one to choose the energy gap as well.

Up to the present time, little work has been done on the quaternary alloys, mainly because work was still being done on ternary (such as $Ga_xIn_{1-x}Sb$), binary (such as GaSb), or elemental semiconductors. Work on the quaternary alloys is basically just the next step in semiconductor research, and it is important to realize that this work rests upon earlier work done on ternary and binary semiconductors.

Chapter II

GROWTH OF THE ALLOYS

2.1 INTRODUCTION

If one is to study an alloy system, the first step is to determine whether single phase material of the desired composition exists. The use of the term "alloy" here is thus more restricted than that in common usage. The alloys one generally speaks of , for example iron alloys, frequently contain several phases intimately mixed, but in the present work, only single phase material is indicated. There is no certain way (short of preparing the material) of determining in advance whether or not single phase alloy material can exist. However, since for all three of the ternary systems $Al_xGa_{1-x}Sb$, $Al_xIn_{1-x}Sb$, and $Ga_xIn_{1-x}Sb$, single phase solid material does exist for all x, there was a reasonable basis for expecting single phase material in the quaternary system. This being so , it was thus decided that it would be worthwhile to continue. In any case, even if there was not single phase material for all x and y, the research would establish the range of x and y for which single phase material did exist.

2.2 PREPARING SINGLE PHASE MATERIAL

The next step is to find a method which will produce single phase material reasonably fast, and in reasonably large amounts. There are several possibilities. One of these is to mix together various amounts of the pure elements or pure antimonides such that the whole sample has the desired average composition , then melt together and cool. This method has been attempted in this laboratory (Ma 72), but it has proven to give unsatisfactory results. The basic problem with this method is that the sample in the liquid state may have the desired composition, but if this sample is cooled, the solid which starts to form when the temperature is low enough (the solid in equilibrium with the liquid) does not in general have the same composition as the liquid (see figure 1). For simplicity, this is illustrated for a binary system, but the same principles apply for a quaternary system. In Ma 72 samples were melted in quartz tubes about 5mm in diameter, then quenched. However, even the fastest quenching possible (a few seconds) still resulted in samples which were non- homogeneous. For this reason, this method was not tried.

In another method samples are prepared as above, but after cooling, the solid is powdered (to about 10 or 20 micron grain size), pressed into another quartz tube, and then annealed at a temperature below the melting point of the

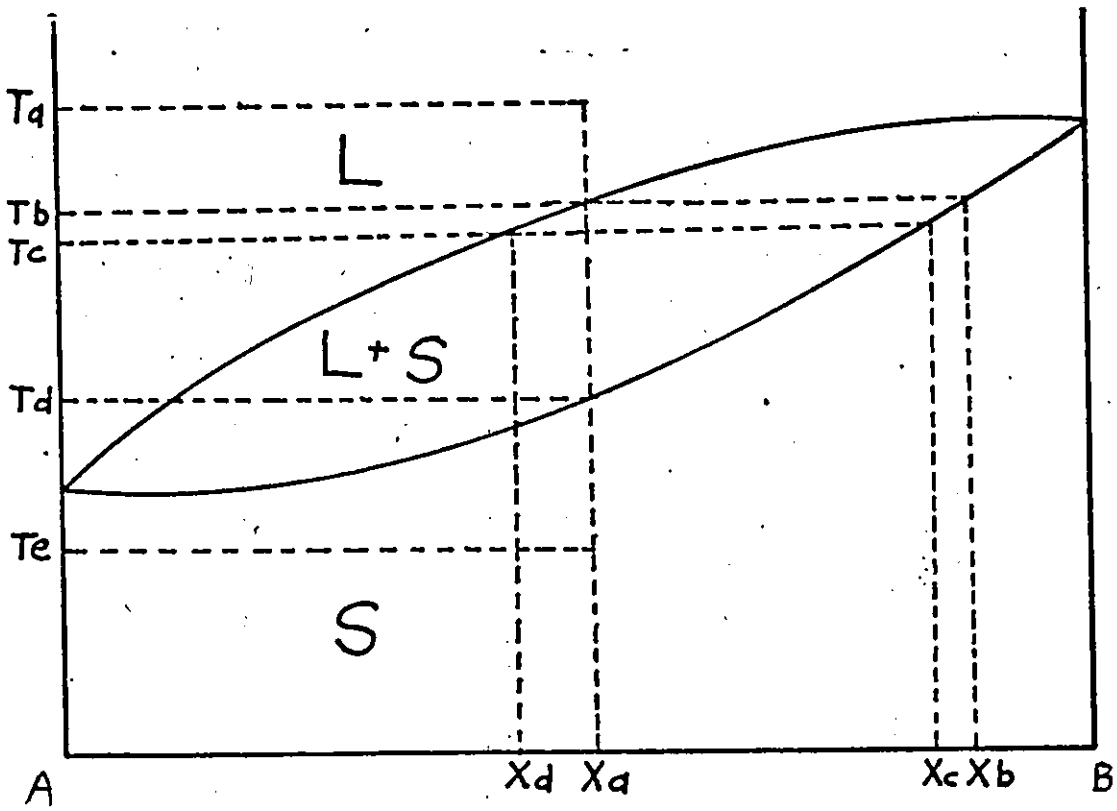

Figure 1: A typical binary phase diagram

A sample of composition Xa has a single liquid phase at Ta and a single solid phase at Te. If it is cooled to Tb, there will be a solid of composition Xb in equilibrium with the liquid. If some solid precipitates out, then the remaining liquid will have a composition Xd, and will start to precipitate out a solid of composition Xc at temperature Tc, and so forth. Thus the cooled sample will not be of uniform composition. To avoid this, the sample must be cooled very quickly from Tb to Td where the equilibrium condition is two phase.

solid, but as close to it as possible. This method was tried for 12 samples, which were then annealed for about 3 months. But even after this period, they had failed to reach equilibrium, so no further attempts were made in this direction.

Directional freezing is still another method, and it was used successfully.It will now be described in detail.

2.3 DIRECTIONAL FREEZING

Directional freezing has been used successfully many times in this laboratory,for example, Martel (Ma 72) prepared $Ga_xIn_{1-x}As_ySb_{1-y}$, Thomas (Th 69) prepared $Ga_xIn_{1-x}Sb$ and others, Gratton (Gr 78) prepared $GaAs_xSb_{1-x}$, and so forth, so it was a logical choice for the particular alloy system being used here. The technique will be described.

A quantity of material (either the pure elements or the pure antimonides) is placed in a quartz tube, then evacuated, and generally backfilled to one half an atmosphere with either argon or nitrogen to facilitate sealing the tube. Quartz is the preferred material because it can withstand high temperatures and sudden temperature changes. Most materials can be sealed directly in quartz, but aluminum compounds will react with the quartz tube causing it to devitrify and eventually break. Thus it is necessary to either coat the inside of the tube with carbon, or place the material in a carbon tube which is placed inside the quartz tube. In the present work,both of these methods were used. The inner carbon tube or the carbon coated quartz tube had an inner diameter of about 10mm and a length of about 15cm. The weight of the charge was generally 30-40 gms. The ma-

terial was then melted in a special furnace which could be rocked during the melting process. The material was rocked in the molten state for a few hours. It was found that this seemed to ensure good mixing and helped to prevent the ingot from breaking up into several smaller pieces along the length of the tube. After melting and cooling, the ingot (still in the quartz tube) was transferred to the directional freeze furnace.

2.3.1 Furnaces

Now, a brief note about the furnaces. The basic furnace consisted of a length of refractory tubing. The length and diameters varied, but a typical tube was 60cm long and 4cm in diameter. Resistance wire is wound on the tube in a coil fashion in order to produce the desired temperature gradient. The wire is then coated with refractory cement to ensure good heat conduction and that the wire stays in place. The tube is mounted centrally along the axis of a rectangular box with aluminum and asbestos board walls, approximately 25cm x 25cm x 60cm. The space inside is filled with vermiculite for insulation. A Pt-PtRh(13%) thermocouple is cemented to the furnce tube near the centre, or placed inside the furnace to be used to control the temperature of the furnace. The directional freeze furnace differs from this. Its main feature is that it is really two furnaces, separated by a three centimeter air gap. Water

cooled copper baffles are placed on either side of the gap. One of these furnaces is heated hot enough to melt the ingot. The other furnace can be heated hot enough to prevent condensation of volatile material when only part of the ingot is in the hot zone of the furnace. This feature wasn't actually required in the present work though. The purpose of the water cooled section is to have as steep a temperature gradient as possible at the end of the furnace. The reason for this will be explained shortly.

The sealed off ingot was placed in one end of a long quartz tube. This end was placed in the hot zone of the furnace, and the other end placed on a trolley which was outside of the furnace. This tube was used merely to hold the ingot and was not sealed off in any way. The trolley was slowly moved along a track, pulling the quartz tube with it, and therefore pulling the ingot out of the hot zone of the furnace. Thus the ingot started to freeze from one end, and eventually the whole ingot was frozen. The ingot was pulled out of the furnace at a rate of 0.8 to 1.5 cm a day, and the whole growing process took 3-4 weeks. Ideally the result is an ingot about 15cm long, 1cm wide, 0.5cm thick and approximately oval in cross section.

2.4 THEORY OF DIRECTIONAL FREEZING

The result of this pulling process is an ingot that has an overall composition gradient, but a thin section of it is single phase and more or less homogeneous. By single phase we mean that an X-ray powder photograph taken of a piece of the thin section shows only one phase (the technique will be explained later). By homogeneous we mean that the change in x and y from one face of the section to another is as small as possible. The sections are about 1mm thick. In practice, homogeneous means that the change in x and y be close to .01, but it may occasionally be several times this. The reason for this will now be considered. As explained earlier using the binary phase diagram, in general for a multicomponent system, as a liquid is cooled , a temperature is reached where the liquid begins to solidify. However, the solid in equilibrium with the liquid at this temperature may not have the same composition as the liquid. Now suppose the liquid contains A and B, but the solid is richer in B than the liquid. This means that the remaining liquid is depleted of some B and it now has a different composition. But this new liquid , at the right temperature, is in equilibrium with a solid of a different composition. Thus , as an ingot solidifies, the composition of the newly forming solid is gradually changing because the liquid is being slowly depleted of B. But, if a section of the ingot is thin relative to the whole ingot, we would not expect much change in composition over the width of the section.

2.5 PROBLEMS OF DIRECTIONAL FREEZING

To grow ingots successfully, one must take into account a number of factors. First, the ingot must be grown slowly enough so that equilibrium conditions are obtained throughout the growing process. We also must have good temperature stability in the furnace (stable to within 1° C, ideally). The temperature gradient at the freezing end must be as steep as possible in order to avoid constitutional supercooling. This results in inhomogeneous solidification at the freezing interface. The reason is because at the liquid-solid interface there is a depletion of the high melting point material (B in my example) which results in a localized drop in the liquidus temperature (the temperature above which there is only a liquid phase). Ideally equilibrium is established by diffusion from the molten part of the ingot. Since diffusion cannot begin until there is a composition gradient established, there is always a localized depletion region and a region of supercooled material is formed immediately in advance of the freezing interface. Generally though, with this method the temperature gradient is steep enough to avoid problems with constitutional supercooling. But if any of these conditions are not met, then all or part of the ingot may be multiphase.

2.6 OBTAINING SLICES

By taking slices from various parts of the ingot, a number of samples with a wide range of composition can generally be obtained. Slices may be taken from the ingot using a variety of methods. In this work three different methods were tried:

1. Spark cutter: A potential difference was established between the ingot and a moving wire. The wire was lowered onto the ingot and the resulting spark eventually cut through the ingot. This method was moderately slow, produced rather bad cuts and suffered from a frequently breaking wire. It wasn't used very much.

2. Wire saw: A thin molybdenum wire, coated with silicon carbide paste, was passed over the ingot until it was cut through. This method was very slow, but the cuts were better, the wire broke less often than in method 1, and thinner slices than in method 3 could be produced.

3. Blade saw: A thin carborundum wheel was used to cut through the ingot. This method was fast, provided good cuts, but the slices had to be rather thick, or they had the tendency to shatter while cutting.

None of these methods were perfect, but generally method 3 was used , and sometimes method 2.

Chapter III

DETERMINATION OF COMPOSITION

3.1 INTRODUCTION

This was probably the most critical aspect of this work, for while the goal was the determination of lattice parameters and energy gaps, it is clearly of little value to know the lattice parameters and energy gaps of unknown materials. It was decided to use an X-Ray fluorescence (henceforward abbreviated XRF) method, as the equipment was convieniently available. A radioisotope XRF method has been used in this laboratory, (Ma 72, Gr 78), but since a working X-ray spectrometer was available, and as the latter was very much more convienient and reliable than the radioisotope setup, it was therefore used.

3.2 THEORY OF XRF

XRF is described in detail in several books (Bi 69, Mu 72) along with details of energy dispersive spectrometers, detectors , etc, so only an outline of the relevent details will be given. Figure 2 illustrates the basic process of XRF. Specifics of samples , crystals, detectors, etc, will follow after an introductory section.

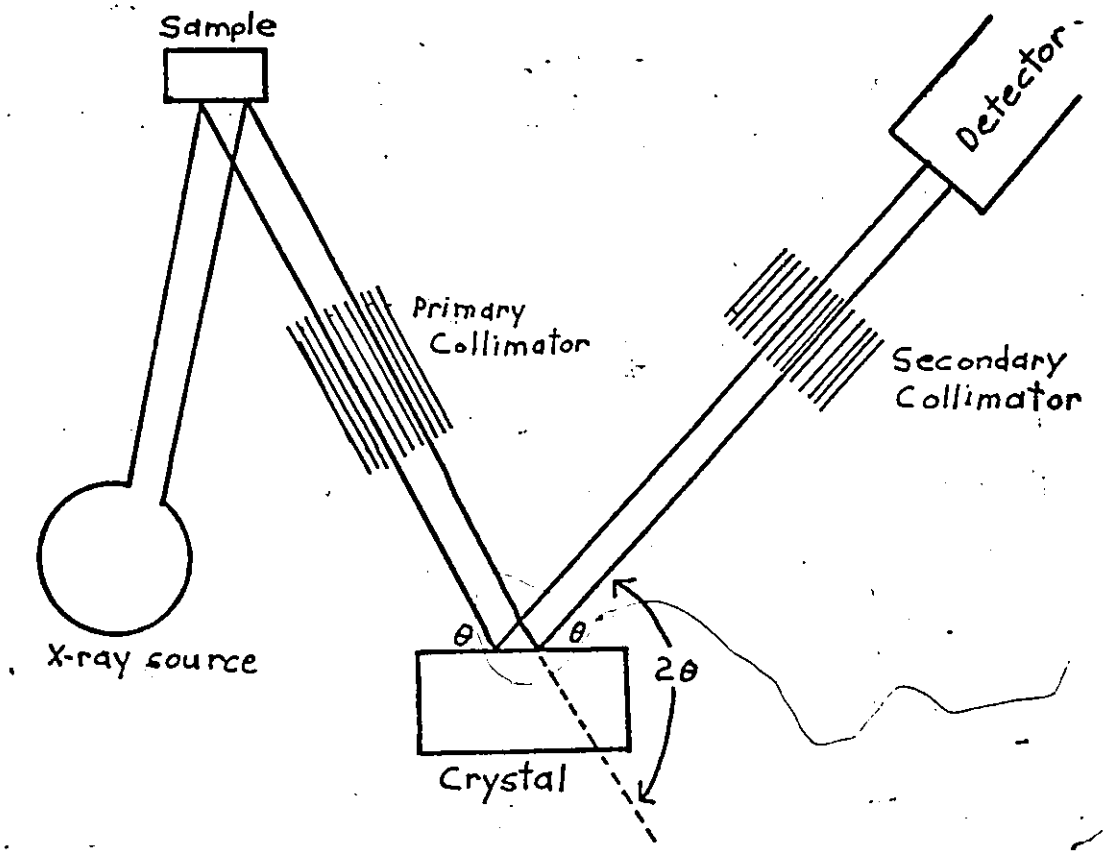

Figure 2: Simplified diagram of an X-ray spectrometer

White X-radiation from the source is incident on the sample. This radiation ionizes some of the inner electrons of the atoms, which results in certain transitions in order to fill these newly vacant energy levels. This radiation causes transitions between inner electron levels in the atoms of the specimen. K-alpha, K-beta, and L-alpha are some typical transitions observed in XRF. In fact, most

practical work makes use of these transitions most of the time, since they are usually the strongest. Since these transitions are between inner electron levels they are effectively independent of the chemical state of the atom, thus the radiation is characteristic of the atom, at least for the heavier elements (Z>6), and serves to distinguish the elements among themselves. By rotating the crystal and detector simultaneously we can detect a given wavelength, hence look for a given element. The detector converts the radiation to counts. So, when we speak of the counts (actually counts/second), we mean the counts recorded from the detector when it is analyzing the characteristic radiation from that element.

3.3 INSTRUMENTATION

The apparatus used to make the measurements basically consisted of two parts: the Phillips PW 1410 X-ray spectrometer, and the Phillips PW 1390 Channel control. There is not really anything special about the spectrometer itself, but, when used with the Channel control, it becomes an instrument of great versatility. The reason is that the Channel control can be programmed to automatically control a series of actions involving the spectrometer, which is not only rapid, but practically eliminates human variability as a factor. The actions which can be controlled include the following:

1. Choice of sample (out of four)

2. Choice of analysing wavelength

3. Choice of length of each measurement

4. Choice of crystal, collimator, and detector for each measurement

The requirements for these measurements were decided after careful study and the measuring program was stored in the Channel control. Once this was done, to make the measurements it was only necessary to load the sample holders. A series of four measurements would take about 22 minutes. The process of XRF will now be considered in greater detail, with particular reference to the various factors which can be controlled by the Channel control.

The spectrometer used a chromium X-ray tube, operated at 60kV and 40mA. The radiation is sent to the sample, which is held in place with one of the sample holders described later. The radiation from the sample, after passing through the primary collimator, in order to obtain parallel radiation, is then diffracted by the crystal. The radiation is diffracted according to the Bragg equation $n\lambda=2d\sin\theta$. The choice of crystal depends on a number of factors. These include the relative intensity of radiation from the crystal, presence or absence of higher order reflections, durability

of the crystal, and of course the value of 2d. The higher the value of 2d, the longer is the maximum wavelength the crystal is capable of analysing. For that reason, analysing the radiation from aluminum required a different crystal. LiF is probably about the best choice under most circumstances, unless light elements need to be analysed.

After being diffracted, the radiation now passes through the secondary collimator. Choice of the secondary collimator controls the resolution of the spectral lines-the narrower the spacing, the better the resolution. However, the intensity of the lines also drops as the spacing is decreased. Two collimators were available, one with a spacing of 250 microns, and another with a spacing of 500 microns.

Two types of detectors were available, a scintillation counter and a flow counter. The flow counter has the same electrical structure as a sealed proportional counter. The latter consists of a metal shell through which passes a central wire, which is insulated from the shell, and is maintained at a high voltage of around 1500-1800 volts. The ends of the shell are sealed with mica or beryllium windows, so that radiation can pass in or out of the shell. The tube is filled with a gas such as Xe, Ar, He, etc to absorb the X-rays and generate electrical pulses, which can be counted. The flow detector differs in that it is built so that gas

can flow in and out of the tube. The principle advantage of this kind of detector is that, since the gas can be replenished, thinner windows (such as mylar), can be used, enabling the detector to be used to detect longer wavelength radiation.

The scintillation counters used for X-ray analysis consist of a thallium iodide activated sodium iodide crystal sealed to the window of a photomultiplier tube which amplifies the signal generated. When an X-ray photon is absorbed in the crystal it generates a number of visible-light photons (scintillations) which may then be counted. The principle advantage of the scintillation counter is that it can be used for detecting the radiation from the heaviest elements. For energies above 6kev it is more efficient than the flow detector, but below 6kev, the noise level is too high for the detector to be useful.

3.4 USING THE COUNTS

(Note: since all exposures were for the same length of time, the counts rather than the counting rate were used. In general, though 'counts' should be replaced by 'counting rate'). The counts for a given element were determined by finding the counts at a particular wavelength (which corresponds to a particular value of 2θ) only, not by integrating over the whole area under the curve of counts vs energy, as

was done for the radioisotope XRF. Since the maximal and integral intensities are proportional for a line (Mu 72), it is only necessary to measure the maximal line intensity. This is what was done. It is practical because the spectrometer used is capable of measuring to the same value of 2θ with a repeatability of $\pm .003'$. This means, in terms of energy, about $\pm$ a few ev. (about 1 part in 10000 or less), so one can be reasonably sure that the same point is measured each time. None of the peaks chosen overlapped with any of the other peaks in the system, so the counts could be used directly. In a system with many more elements, the analysis can get quite complicated because of the overlapping peaks. However, this does not concern the present analysis.

In addition, for each element a point was chosen to determine the background counting rate, which was subtracted from the peak rate. In practice it appears that little , if any accuracy is lost by assuming that the background is a constant, finding an average value of this from a series of measurements, and using this value in subsequent calculations. The background point was also far enough away from any of the peaks that there was no interference from them.

To ensure repeatability of the measurements, in addition to counting at the peak and subtracting the background, use was made of a normalizing standard. This was an additional

sample which contained all of the elements present in the other samples. Its composition was not known, but this was not important. It was only necessary that about equal amounts of all the elements be present. The normalizer was analyzed within minutes of analyzing the other samples, as frequently as once every 3 unknown samples (the spectrometer can hold a maximum of 4 samples at a time), but once a day was usually sufficient. The counts from the normalizer at a particular angle are compared with the counts obtained from the initial analysis of the normalizer at the same angle. Ideally,then, all the counts are then adjusted up or down according to whether the normalizer counts are higher or lower than they were the first time. For example, if the antimony peak of the normalizer was originally giving 1000 counts/sec, but at a later date it was only giving 900 counts/sec, then all the measurements of the antimony peak made at that time would be considered to be only 90% of their "true" value, and raised accordingly. Thus, any changes in the system we would expect to be evident in the changes in the normalizer, since we use the same normalizer each time. Changes in the normalizer are small and slow, and unless they were significant, the results from the normalizer were generally ignored. However, it must be considered. It proved necessary in the present case. From June 1979 to April 1980, the antimony peak dropped to 96% of its original level, indium to 97% , and gallium to 80%. The

drops were quite gradual, the day-to-day changes being insignificant. In the case of the gallium peak, it proved to be necessary to make such a large adjustment in order for the sample measurements made in June agree with those made in April. In view of this fact, a change in the normalizer can be ruled out. One possible explanation for this change is that the X-ray tube may have changed with time. Observations of other X-ray tubes in operation confirm this view. Also, the response of the detectors may have changed with time, or some other subtle factor may be involved.

TABLE 1

Summary of the XRF measurements

Element	Line analysed	Peak angle	Backgrnd angle	Detector	Collimator	Crystal
Sb	Kα (2nd order)	27.00	28.00	Scintillation	Coarse	LiF 200
In	Kα (2nd order)	29.46	31.80	Scintillation	Coarse	LiF 200
Ga	Kα	38.88	37.00	Scintillation	Coarse	LiF 200
Al	Kα	144.98	140.00	Flow	Coarse	PE

Coarse collimator spacing: 500 microns
Crystals: LiF (200) plane 2d= 4.02 Å
PE (pentaerythratol) (002) plane 2d= 8.76 Å

3.5 SAMPLE PREPARATION AND SAMPLE HOLDERS

Since this subject is thoroughly discussed elsewhere (Mu 72 for example), only a few relevent details will be considered.

There are 3 main principles that must be considered when preparing samples for XRF analysis:

1. homogeneity
2. grain size, and
3. surface preparation

Given that the counts from an unknown specimen are known, determining the composition is not a trivial matter since the intensity of an X-ray wavelength leaving the sample (hence the counts or counting rate at a particular angle) depend not only on the relative amount of the element which gives this particular wavelength, but also on the relative amounts of all the other elements. This is because while all elements may absorb the characteristic radiation from an element, they would not do so to the same degree. Some elements may even enhance the radiation from another element. To determine the composition of something by chemical analysis means that the sample is destroyed, and the constituents isolated. Thus it makes no difference how the components of

the sample were arranged. However, for a sample used for XRF, the situation is entirely different, because the sample is unaffected by the measurements. For one thing, a large sample may be used, but the X-rays do not penetrate into the sample very much, only about 100-300 microns. Thus only a comparatively small amount of material is being analysed. To ensure that this small part is representative of the whole sample, it must be homogeneous. For the XRF results to be meaningful, the path of all X-rays entering or leaving the sample must be the same, that is, every X-ray must "see" the same number of atoms of each different element, so that absorption is independent of position in the sample. This is accomplished if the sample is homogeneous on a scale considerably smaller than the penetration depth of the X-rays, which, as mentioned earlier, was about 100-300 microns (but note that radiation from a very light element in a heavy matrix can have considerably smaller penetration depths). In practice (see, for example, Ca 66) this means homogeneity on a scale greater than about 10 microns. This means that any volume in the sample greater than or equal to about (10 microns)^3 in size must contain the same quantity of each element as any other equal volume, but any volume less than this need not. In practical terms, for the various factors mentioned, this may be considered as follows:

1. homogeneity-this would be as discussed as above.

2. grain size-the sample could consist of a mixture of several kinds of powder, but provided that all the powders had grains no larger than about 10 microns, the results would be unaffected by grain size

3. surface preparation-provided surface irregularities were no larger than about 10 microns, the condition of the surface would not matter.

Using these principles, one comes up with 4 main ways of preparing samples:

1. liquid solution

2. borax (or other) glass fusion

3. powdered and pressed samples, with or without a binder

4. solid sample with a smooth surface

Methods 1 and 2 were not used. Most of the standards were prepared by method 3. In this method, the samples to be used were powdered, and a quantity of each was weighed, mixed with a weighed quantity of a binder, and pressed into a pellet about 3mm in diameter under a mass of about 400kg. It is not necessary to use a binder (the binder used was phenolformaldehyde, an organic resin), but without a

binder, the powder tends to flake off the pellet, and it eventually crumbles in most cases. Since it is undesirable to introduce powder into the spectrometer, use of a binder is the preferred method. The pellets can be made even more durable by heating them at around 100°C for an hour, which makes them less brittle It is not necessary for all the pellets to be the same thickness, provided they were thicker than 500 microns or so (greater than the penetration depth of the X-rays). To make one of these pellets, no more than 15-20mg of material needs to be used, which is a considerable advantage. However, it is rather time consuming to weigh and powder the samples.

Since samples were to be cut into slices (slices from the directionally frozen ingot) anyways, and since the surfaces of the slices were reasonably smooth, most of the samples were analyzed using method 4. This made the preparation process simple and quick, since one only needed to ensure that the surface was clean and flat enough. Once this was done, the sample could be used directly. Note that method 4 may be considered as a special case of method 3 (without any binder) since powders with a grain size of the order of 10 microns give the same results as a solid. There was no appreciable difference in the values of the composition determined whether binder was used or not.

3.6 SAMPLE HOLDERS

The sample holders were made out of pure (commercial grade) copper, in order that the radiation from the elements in the sample holder would not interfere with the radiation from the sample elements. However, if this could not have been avoided, it would have been possible to filter out the copper radiation. 2 types of sample holders were constructed, one type (figure 3b) for holding the pressed pellets, and a second type (figure 3c) for holding the slices. As the spectrometer was designed for much larger samples, the new holders had to fit inside the original ones (figure 3a). It was also necessary to preserve the geometry of the original holders, in order that the samples would be the same distance from the X-ray beam as samples used in the original holders would. Further details concerning sample preparation and holders may be found in Mu 72.

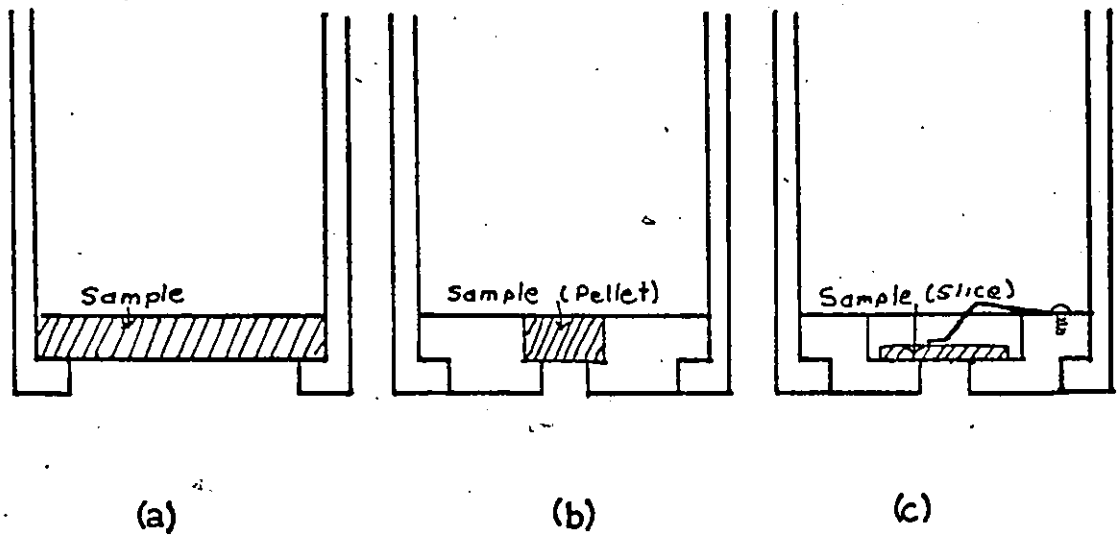

Figure 3: Sample holders

3.7 THE LACHANCE EQUATION

Now that we have established the method of determining the counts from a specific element, and the way the measurements were made, we need to establish some way of relating the counts to the composition, since the counts are not simply proportional to the amount of one element. A method has been devised by Lachance, which appears to give good results, and was used in the present analysis. Lachance's method (La 66#1, La 66 #2) may be summarized as follows:

The relative intensity of a characteristic line emitted by a multicomponent system may be computed from the relationship:

$$\frac{Ia}{I(a)} = \frac{Ca}{1+Cb\alpha ba+Cc\alpha ca.....+Cn\alpha na} \qquad (1)$$

where Ia= net measured intensity of X-ray line A from a specimen.

I(a)= net measured intensity of X-ray line A from pure element A.

Ca,Cb..... are weight fractions of elements A,B,.....

αab, αac ....are constants that account separately for the effects on the intensity emitted by element A caused by elements B,C etc.

The method is found to be applicable to X-ray diffraction XRF, and electron microprobe analysis.

There may be some question as to why weight fractions have been used, rather than atomic fractions, since the various factors would seem to depend on the relative numbers of the different elements, rather than the relative weights. The reason is that the method was developed for purposes (compositions of rocks, ores,etc) where the weight fraction was the item of interest. It was decided to preserve the form of the Lachance equation, and convert from weight to atomic fractions after the composition determination, because his was a proven method. Also, since the chemical formula of the binder wasn't known, the atomic fraction of the binder could not be established anyway.

3.8 TERMINOLOGY

The following terms and abbreviations will be used in the remainder of this work.

a=Al

g=Ga

i=In

s=Sb

b=Binder

αba, αca ....are constants that account separately for the effects on the intensity emitted by element A caused by elements B,C etc.

Wx= atomic fraction of element X in the sample

Wox= weight fraction of element X (or Binder) in the sample

Cx= counts at the characteristic line peak of element X in the sample

C100x= counts at the characteristic line peak of element X in pure X

C100yx= counts at the characteristic line peak of element X in the pure compound y (in this case, only antimonides)

Define Ka, Kg, Ki such that

Wos = KaWoa in pure AlSb

Wos = KgWog in pure GaSb

Wos = KiWoi in pure InSb

These numbers were calculated and are:

Ka = 4.5127 Kg = 1.7465 Ki = 1.0602

so, in a mixture of pure antimonides, this relation holds true:

$$Wos = Woa*Ka + Wog*Kg + Woi*Ki$$
$$= 4.5127*Woa + 1.7465*Wog + 1.0602*Woi \qquad (2)$$

Since all samples were analyzed for the same length of time (40 seconds) and each sample had an equal area exposed to the beam, as well as being exposed to the same position in the beam, and were smooth and homogenous enough to be unaffected by these factors, then the only variables affecting the counts are the relative amounts of the various elements.

So we can write

$$Ia/I(A) = Cx/C100x$$

Rewriting Lachance's equation with this terminology,

$$\frac{Cx}{C100x} = \frac{Wox}{1+\sum_{i\neq x}^{n} \alpha ix Woi} \qquad (3)$$

or (where there are n elements i)

$$\frac{C100x}{Cx} Wox - 1 = \sum_{i\neq x}^{n} \alpha ix Woi \qquad (4)$$

where the α's are constants.

In principle we can write exactly,

$$\frac{C100xWox}{Cx} - 1 = \sum_{i \neq x}^{n} \sum_{j=1}^{\infty} \alpha jix (Woi)^j \qquad (5)$$

But Lachance (La 70) has shown that there is little value in including higher order terms, keeping only the single term (j=1) is a very good approximation. No attempts were made to determine higher order terms.

3.9 DETERMINATION OF THE α COEFFICIENTS

In principle, one can obtain the α coefficients from series of two-element mixtures, but this has its difficulties, because ensuring homogeneity by careful powdering would be next to impossible with, for example, indium-gallium mixtures. It was decided instead to obtain the coefficients from mixtures of the antimonides, since such samples had already been made for annealing purposes.

The pure antimonides were accurately weighed out, melted together, quenched, powdered, mixed well with an approximately equal (but known) weight of binder, and pressed into pellets. A total of 12 samples, with a wide range of average compositions, were prepared in this way. The samples

were multiphase, but were powdered and mixed well enough, in my opinion, so that X-ray analysis would give a true average composition. In addition, the pure antimonides and the pure elements were made into pellets of the same size. A series of binder+ single antimonide pellets were also prepared, since the binder absorbs radiation, and we must therefore define α_{bx} coefficients (but of course there are no α_{xb} coefficients).

Counts were obtained for the various elements in all of the samples. It turned out that the aluminum counts were quite low (of the order of one tenth that of the other elements), so it was decided not to use them, for the sake of accuracy. It is not necessary to know the aluminum counts, however, since there are 3 pieces of information (Sb, In, and Ga counts), even without the aluminum counts, but only 2 unknowns (x and y).

Values of C100x were obtained from analysing the pure elements. From analysing the pure antimonides, since we just have two-element pairs, it is easy to obtain α_{xs} and α_{sx}. By analysing the series of pellets which contained only binder and pure antimonide, we may graphically obtain α_{bx} and α_{sx}. Note that we may obtain the α_{sx} by two different methods. Similar results are obtained for both these methods. Now this leaves only 4 unknowns to find from the

analysis of the 12 mixed antimonide + binder data: αgi, αig, αai, and αag. Pairs of these unknowns may be easily found graphically. Details of the graphical analysis follow.

3.10 GRAPHICAL ANALYSIS OF THE DATA

1. Analysis of the pure antimonide data.

Using equation (4), since there is only one unknown, we can write

$$\frac{C100sWos}{Cs} - 1 = \alpha sx Wox \qquad (6)$$

and find αxs directly. We can use a similar procedure , replacing the antimony counts with those of the other element, to obtain the αsx.

2. Analysis of the binder + single antimonide data. First consider the equations derived from the antimony counts. Using equation (4), we can get three equations of the form

$$\frac{C100sWos}{Cs} - 1 = \alpha xs Wox + \alpha bs Wob \qquad (7)$$

where x can be a, g or i. But note that Wob= 1- Wos-Wox. (8)

Also, Wos = Kx*Wox (eqn(2))

So we can now write

$$\frac{Wos}{Cs} = \frac{Wos}{C100s}(Kx\alpha xs - \alpha bs(Kx+1)) + \frac{1 + \alpha bs}{C100s} \qquad (9)$$

Thus, if we plot Wos/Cs vs Wos, we should get a straight line with slope

$$\frac{Kx\alpha xs - \alpha bs(Kx+1)}{C100s}$$

and intercept

$$\frac{1 + \alpha bs}{C100s}$$

Since we know C100s, we can therefore obtain αxs and αbs.

If we now consider the equations obtained from the counts of x (Al, Ga, and In), we get

$$\frac{C100xWox}{Cx} - 1 = \alpha sxWos + \alpha bxWob \qquad (10)$$

and making use of equations (2) and (8), we obtain

$$\frac{Wox}{Cx} = \frac{Wox}{C100s}(\alpha sxKx - \alpha bx(1+Kx)) + \frac{1 + \alpha bx}{C100s} \qquad (11)$$

By plotting Wox vs Wox/Cx, we again obtain a straight line, and we can obtain the αsx and αbx from the slope and the intercept.

3. Analysing the binder + mixed antimonide data. From equation (4) we can set up 4 equations, one for each of Ca, Cg, Ci, and Cs.

$$\frac{C100aWoa}{Ca} = 1 + \alpha gaWog + \alpha iaWoi + \alpha saWos + \alpha baWob \qquad (12)$$

$$\frac{C100gWog}{Cg} = 1 + \alpha agWoa + \alpha igWoi + \alpha sgWos + \alpha bgWob \qquad (13)$$

$$\frac{C100iWoi}{Ci} = 1 + \alpha aiWoa + \alpha giWog + \alpha siWos + \alpha biWob \quad (14)$$

$$\frac{C100sWos}{Cs} = 1 + \alpha asWoa + \alpha gsWog + \alpha isWoi + \alpha bsWob \quad (15)$$

Since we now know the αxs, αsx, αbx, Wox's, C100's, and C's each equation has only two unknowns. Rewriting the first 3 equations as follows,

$$\left(\frac{C100aWoa}{Ca} - 1 - \alpha saWos - \alpha baWob\right)/Wog = \alpha ia\frac{Woi}{Wog} + \alpha ga \quad (16)$$

$$\left(\frac{C100gWog}{Cg} - 1 - \alpha sgWos - \alpha bgWob\right)/Woa = \alpha ig\frac{Woi}{Woa} + \alpha ag \quad (17)$$

$$\left(\frac{C100iWoi}{Ci} - 1 - \alpha siWos - \alpha biWob\right)/Woa = \alpha gi\frac{Wog}{Woa} + \alpha ai \quad (18)$$

we can easily see that these are linear equations , and the unknown coefficients may be obtained from the slope and intecept.

Thus we have found all the unknown quantities. The results for all the analyses are summarized in table 2.

TABLE 2

The α coefficients and the C100's			
$\alpha ag = .68 \pm .13$ $\alpha ig = .94 \pm .06$ $\alpha sg = 1.16 \pm .15$ $\alpha bg = -.67 \pm .06$	$\alpha ai = -.67 \pm .06$ $\alpha gi = .00 \pm .03$ $\alpha si = -.26 \pm .01$ $\alpha bi = -.75 \pm .03$	$\alpha as = -.84 \pm .04$ $\alpha gs = -.25 \pm .01$ $\alpha is = -.15 \pm .01$ $\alpha bs = -.72 \pm .03$	C100g=945,000 ± 2% C100i=120,300 ± 2% C100s=102,500 ± 2%

3.11 COMPARISON OF THEORY WITH EXPERIMENTAL DATA

Now, using these α's and C100's, we can go back and calculate the composition, to see how well the compositions determined using these quantities agree with the actual compositions. Since we have 3 pieces of information, Cg, Ci, and Cs, but only 2 unknowns, x and y, we can use any 2 of the counts, along with the α's, to determine the composition. Similar results are obtained when any pair of counts are used. As an example, the results obtained when only the indium and gallium counts are used may be seen in table 3.

TABLE 3

Comparison of compositions determined from the α coefficients with the actual compositions

T-theoretical compositions obtained from the computed α's, the C100's, and the indium and gallium counts.
E-actual compositions of the samples

(numbers are atomic fractions)

Sample #	AlSb		GaSb		InSb	
	T	E	T	E	T	E
1	.171	.200	.721	.700	.107	.100
2	.693	.700	.104	.100	.204	.200
3	.246	.250	.448	.450	.305	.300
4	.269	.300	.312	.300	.418	.400
5	.041	.050	.107	.100	.853	.850
6	.108	.100	.152	.150	.740	.750
7	.033	.050	.307	.300	.659	.650
8	.123	.100	.281	.300	.596	.600
9	.231	.210	.158	.160	.611	.630
10	.238	.250	.047	.050	.715	.700
11	.353	.350	.056	.050	.590	.600
12	.093	.100	.350	.350	.556	.550

The accuracy obtained is comparable with that obtained by Lachance (La 66#1, La 66#2), and by Birks (Bi 69), who used a similar method.

3.12 COMPOSITION DETERMINATION

To determine the composition, given that the counts are known, requires solving a system of linear equations. A faster way is to simply prepare a table of counts as a function of composition, and merely consult this table to find the composition. This enables compositions to be determined "on the spot". One set of samples could have their compositions determined before the next set was analysed, which was convienient, since it sometimes enabled one to get by with analysing fewer of the samples. A still better technique is to prepare a set of ratios (Cg/Cs , Cg/Ci, or Ci/Cs) as a function of composition. By using ratios, the effect of surface preparation grain size, area of sample exposed, etc, can be reduced even further, since while radiation intensity is a strong function of these factors, the ratios are relatively constant. This was true even for gross differences. Most of the compositions were determined from tables of Cg/Cs and Ci/Cs, derived from the α's and C100's. Table 4 gives an abbreviated version of these tables, to give an idea how these ratios varied. (the actual tables used had listings for about every 1% difference in composition).

TABLE 4

Count ratios as a funcion of composition				
Atomic fraction				
AlSb	GaSb	InSb	Cg/Cs	Ci/Cs
0.000	0.000	1.000	0.000	1.184
0.000	0.200	0.800	0.487	0.950
0.000	0.400	0.600	1.000	0.714
0.000	0.600	0.400	1.543	0.478
0.000	0.800	0.200	2.126	0.240
0.000	1.000	0.000	2.758	0.000
0.200	0.000	0.800	0.000	0.966
0.200	0.200	0.600	0.482	0.728
0.200	0.400	0.400	0.990	0.487
0.200	0.600	0.200	1.531	0.245
0.200	0.800	0.000	2.115	0.000
0.400	0.000	0.600	0.000	0.743
0.400	0.200	0.400	0.475	0.498
0.400	0.400	0.200	0.978	0.251
0.400	0.600	0.000	1.516	0.000
0.600	0.000	0.400	0.000	0.511
0.600	0.200	0.200	0.467	0.258
0.600	0.400	0.000	0.963	0.000
0.800	0.000	0.200	0.000	0.266
0.800	0.200	0.000	0.457	0.000
1.000	0.000	0.000	0.000	0.000

3.13 RELIABILITY OF THE COMPOSITION DETERMINATION

The strongest evidence that the compositions are as claimed is that the set of α coefficients produces reasonable agreement with experiment when these coefficients are used with the known counts of the 12 standard samples. This is especially true considering that only 4 of the 12 α's were actually determined from the standards data, the others coming from the pure element and antimonide data, as well as from the pure antimonide+ binder data. Additional evidence will be given later in this work.

3.14 COMPOSITION OF THE UNKNOWN INGOTS

The ingots, prepared by the directional freezing method described earlier, had approximately 1mm thick slices taken from them about every 1cm along the length of the ingot, using one of the methods described earlier. The counts were determined, the ratios Cg/Cs and Ci/Cs were found and the composition of the slices were found by consulting the tables. From these results, the region of the ingot which had a significant positive aluminum concentration was found, and this section was then sliced up completely into 1mm thick slices, and every slice was analysed. Next, the atomic fractions of AlSb and GaSb were plotted as a function of composition. It was decided to draw a smooth curve through these points and to use these curves, not any particular point, to determine the composition at any distance along the ingot. There are good reasons for this. We note that any particular point on the graph is subject to uncertainty for the following reasons:

1. statistical error in counts

2. measuring error in position of slice on the ingot

3. additional error in position of slice, because no attempt was made to note which side of the slice was analysed. This means that there is an additional uncertainty of 1mm in the position.

4. uncertainty in the α's

The smoothing procedure would tend to eliminate the first 3 of these sources of error. This smoothing procedure was also used for the lattice parameter and energy gap data.

3.15 EVIDENCE OF RELIABILITY OF THE COMPOSITION DATA

If the composition data is reliable, then, given that the composition vs distance curve is known for the ingot, as well as the length of the ingot, then it should be possible to deduce the starting composition of the ingot and find that it agrees with the known starting composition. This is true if the following conditions hold:

1. each slice has the same area
2. there was no loss of material during the growing process
3. there was no multiphase region in the ingot (this could mean lack of homogeneity, thereby preventing the true composition from being known).

This can be accomplished by integrating the curve of composition vs distance, then dividing by the total length of the ingot, which should give the fraction of the particular material which makes up the ingot. This was done as well as possible, and the result was compared with the known starting compositions. The results may be seen in table 5.

TABLE 5

Ratios of Theoretical/actual starting compositions of the ingots		
Ingot	% AlSb accounted for	% GaSb accounted for
104545#2	104	101
201070	73	101
161668	78	89
252550	106	88

Results are expressed as the ratio of the calculated atomic fraction / the actual atomic fraction (of the starting ingot). These results appear reasonable, considering that the 3 conditions mentioned didn't hold exactly for any of the ingots.

The following pages contain the graphs of composition vs distance along ingot, as well as graphs showing the composition of the ingots plotted using triangular coordinates. We see from graphs 2-5 that the ingots typically start rich in aluminum, and the aluminum concentration drops rapidly to near zero. Since the ingots are 12-15cm long, much of each ingot has negligible aluminum in it. This is not unexpected, since the components of this system have a wide difference in melting points. No general remarks may be made about the variation of the GaSb concentration. This would depend on the phase diagram, which is not presently known. The difference in melting points of InSb and GaSb is too small (about 200 degrees) for any general remarks to be

made in the absence of more information. As mentioned earlier, some of the ingots, after solidification, were not in one long piece, but in several smaller ones. Graphs 1 and 2 show examples of such ingots. In each of these cases, the piece which was the second to freeze was used in the analysis (identified by #2 after the ingot identification symbol). These pieces were chosen because they were relatively long and had regions of significant AlSb concentration. The length of these pieces was about 6cm, so the region of significant AlSb concentration was considerably less than in the other ingots. Ingot 104545 broke into two pieces of aproximately equal length, and it is believed that they had much the same composition. The starting composition of Ingot 103060#2 was not known, so it is difficult to say whether the pattern of Ingot 103060 follows the same pattern as the other ingots (high initial AlSb concentration, falling rapidly). This pattern is more obviously seen by examining graphs 6-10. In all the graphs, only the regions with a significant AlSb concentration are shown, which is only about one quarter to one third of the whole length of the ingot. In addition, smooth lines were drawn only through the regions of the ingots that were not multiphase, since useful information on the other measured parameters could be obtained only when the samples were single phase. Graphs 2-4 have such multiphase regions. For those unfamiliar with triangular coordinates, the atomic fraction of one

of the 3 antimonides may be found by determining the fraction of the distance along the perpendicular bisector from one edge of the triangle to the opposite corner. The corners represent the pure antimonide (see figure 4). The information on graphs 1-5 is presented in graphs 6-10 in order that it may be quickly seen where the compositions of the ingots lie in relation to the entire alloy system.

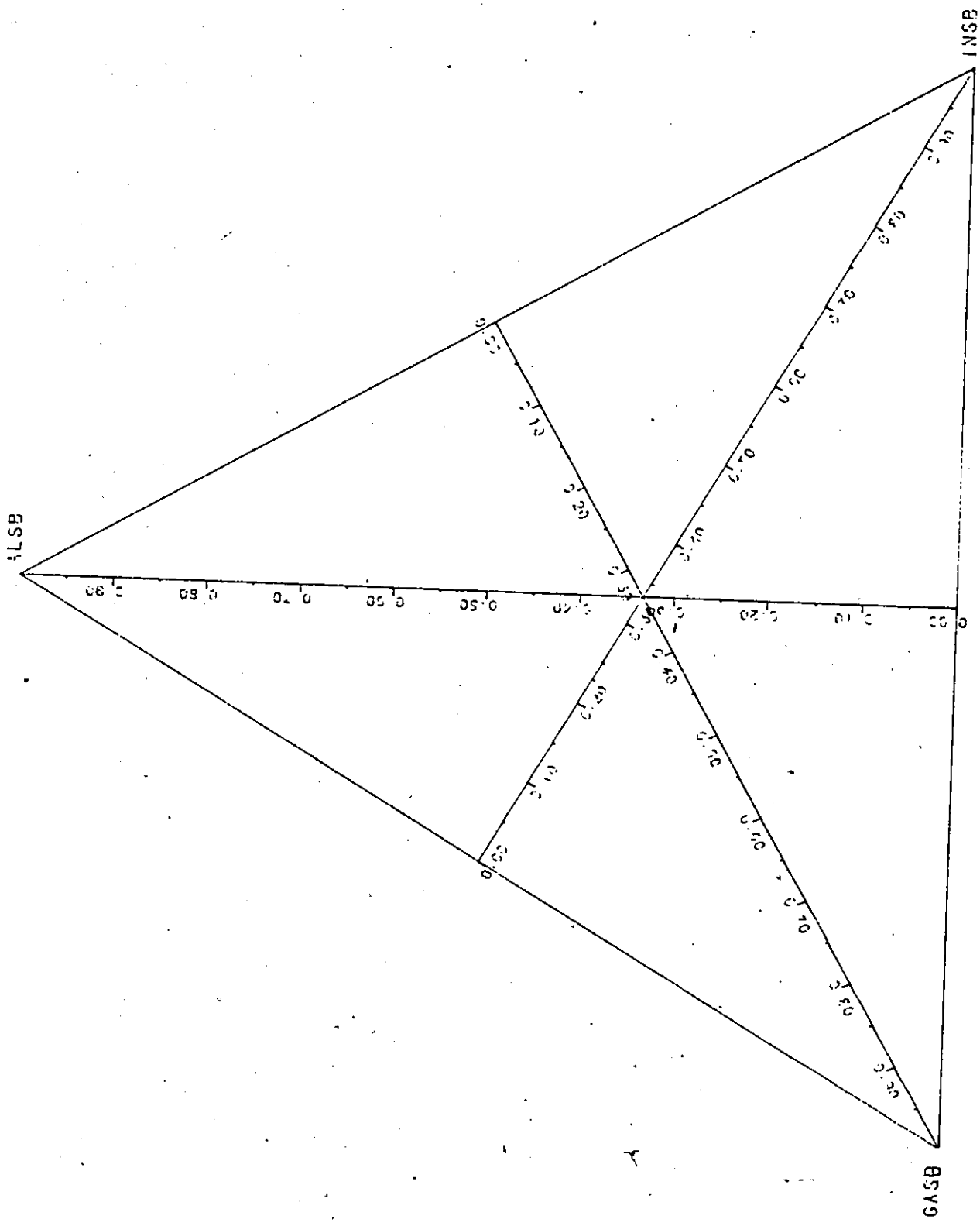

Figure 4: Triangular coordinates

Graph 1: Composition vs distance for
Ingot DF Agis 103060#2

Graph 2: Composition vs distance for
Ingot DF AGIS 104545#2

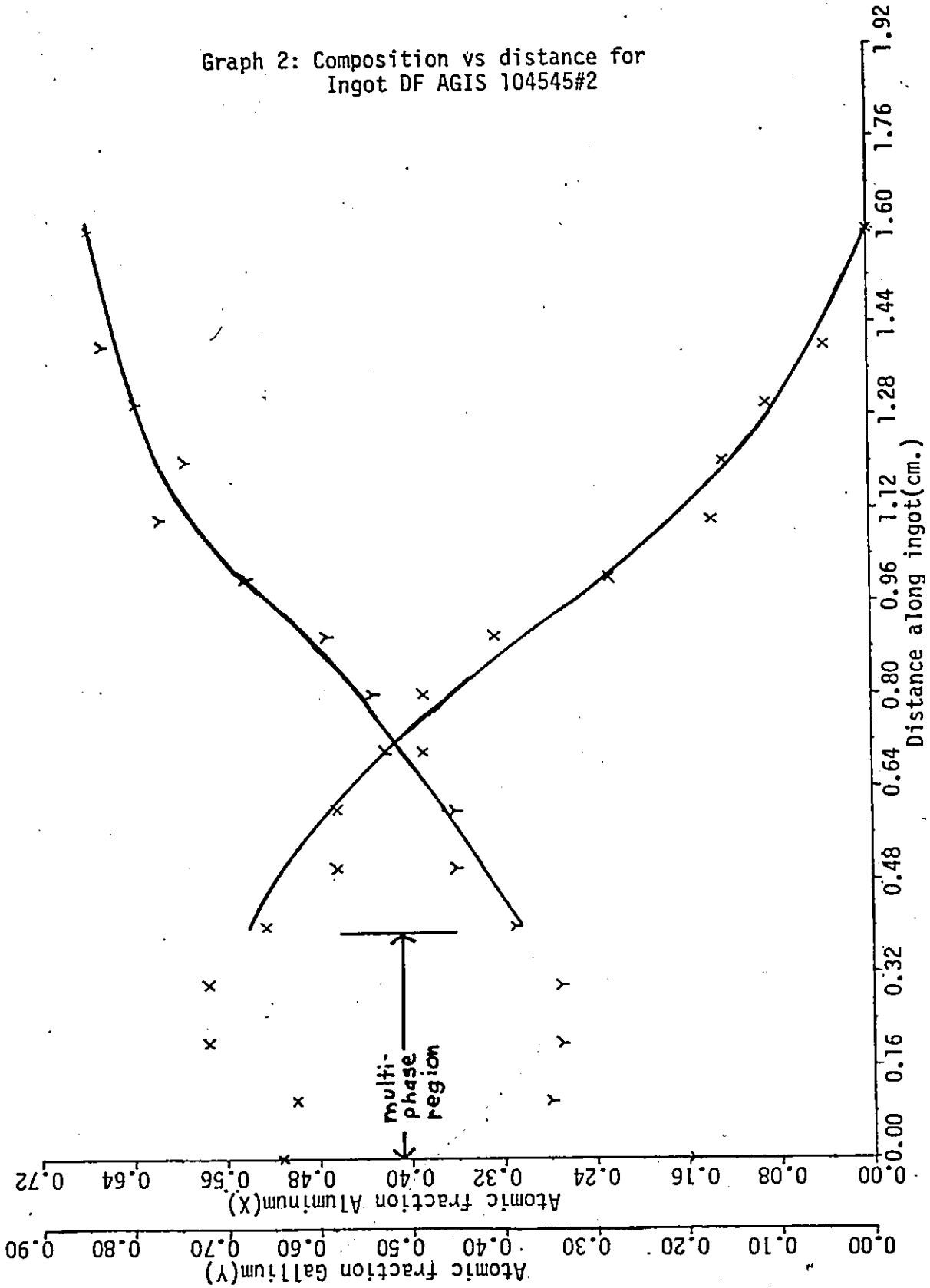

Graph 3: Composition vs position for
Ingot DF AGIS 161668

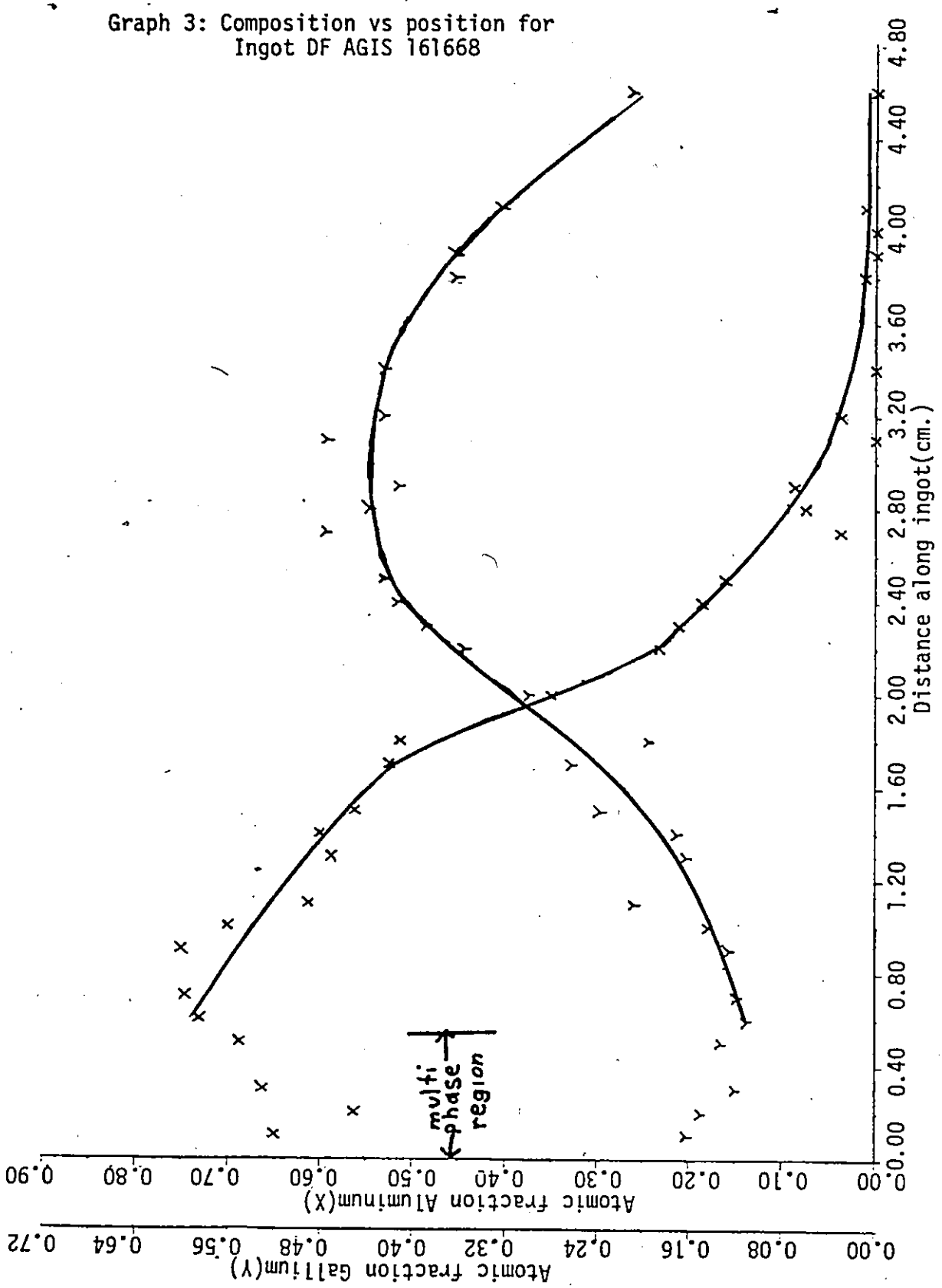

Graph 4: Composition vs distance for
Ingot DF AGIS 201070

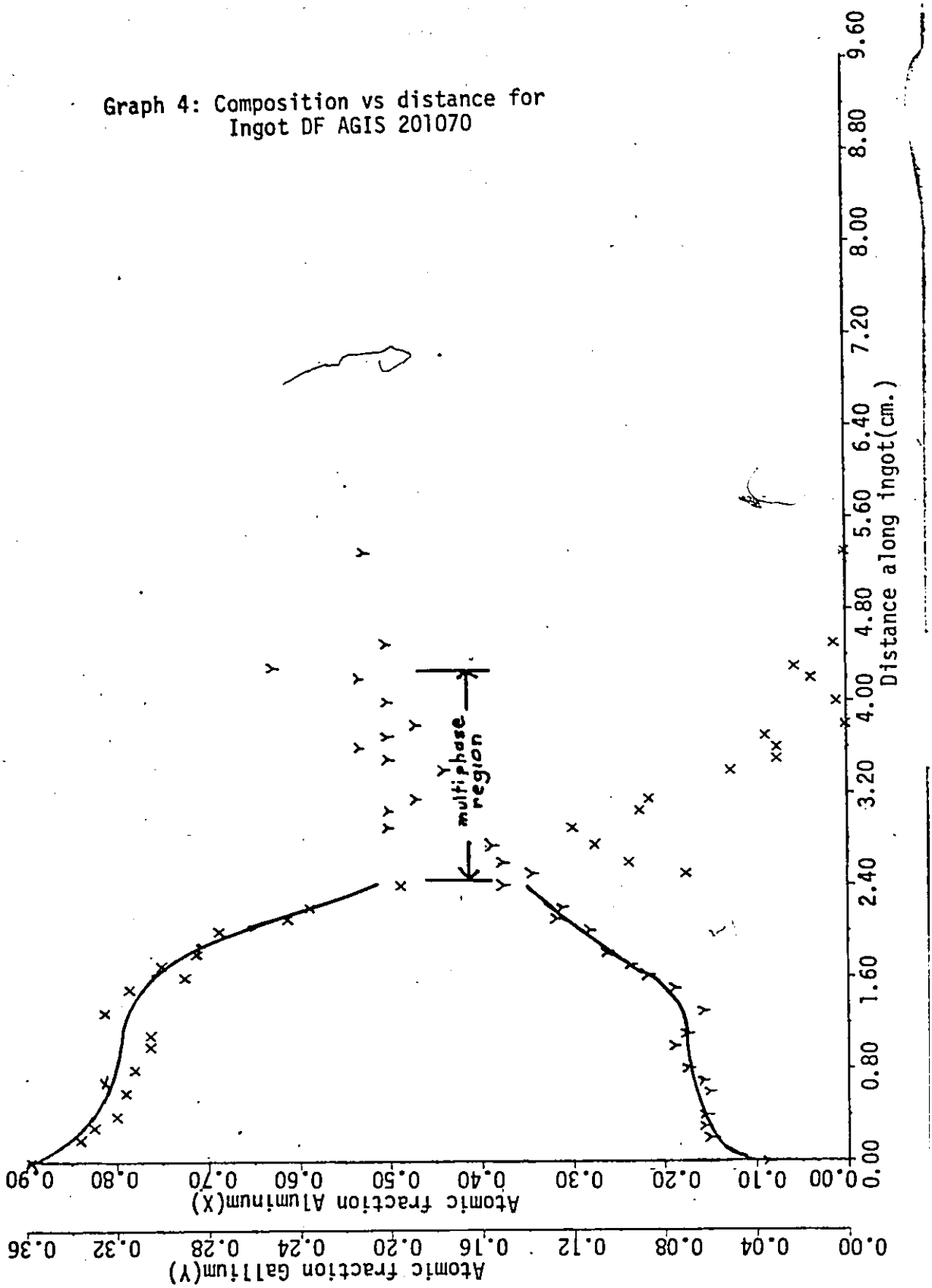

Graph 5: Composition vs distance for
Ingot DF AGIS 252550

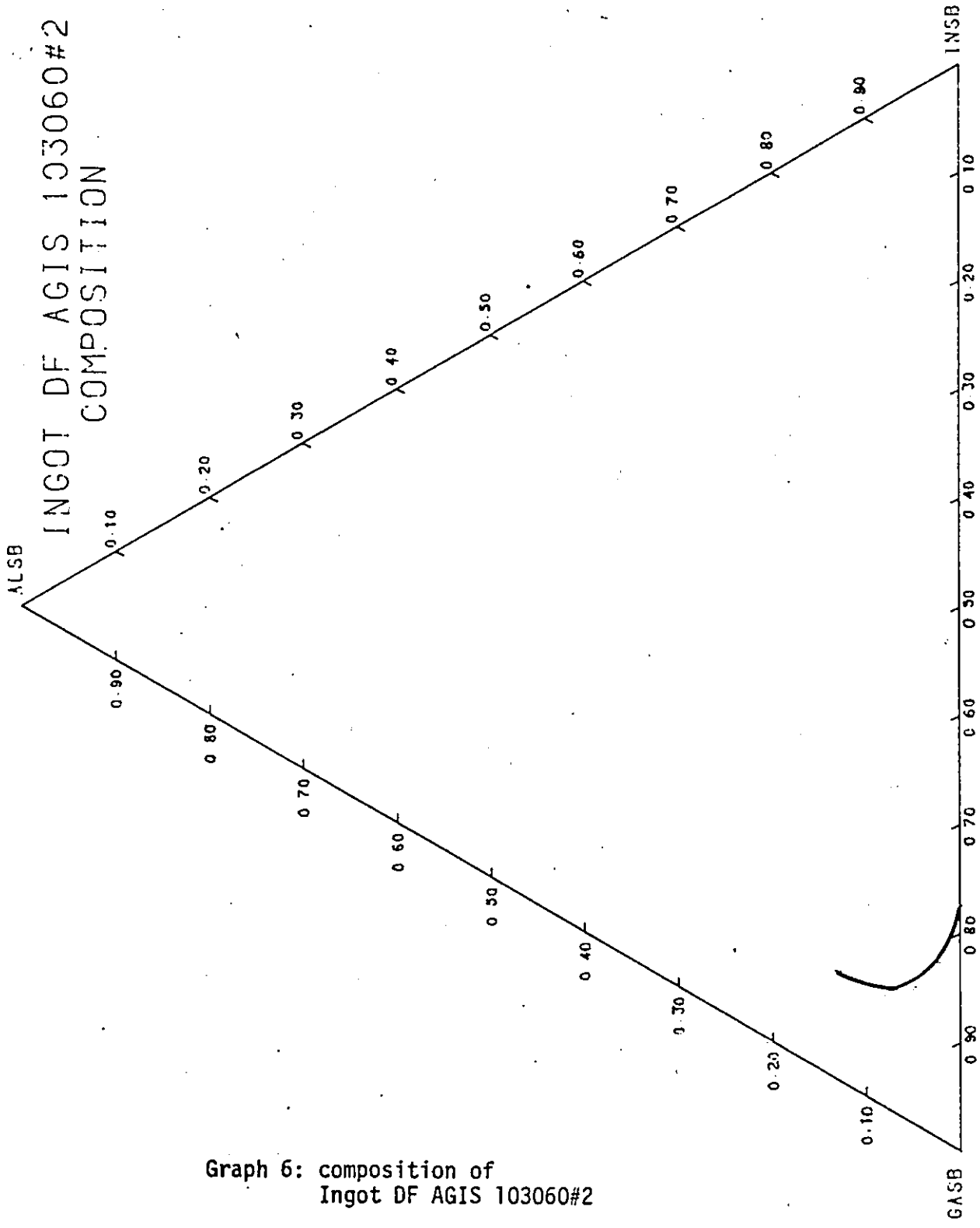

Graph 6: composition of
Ingot DF AGIS 103060#2

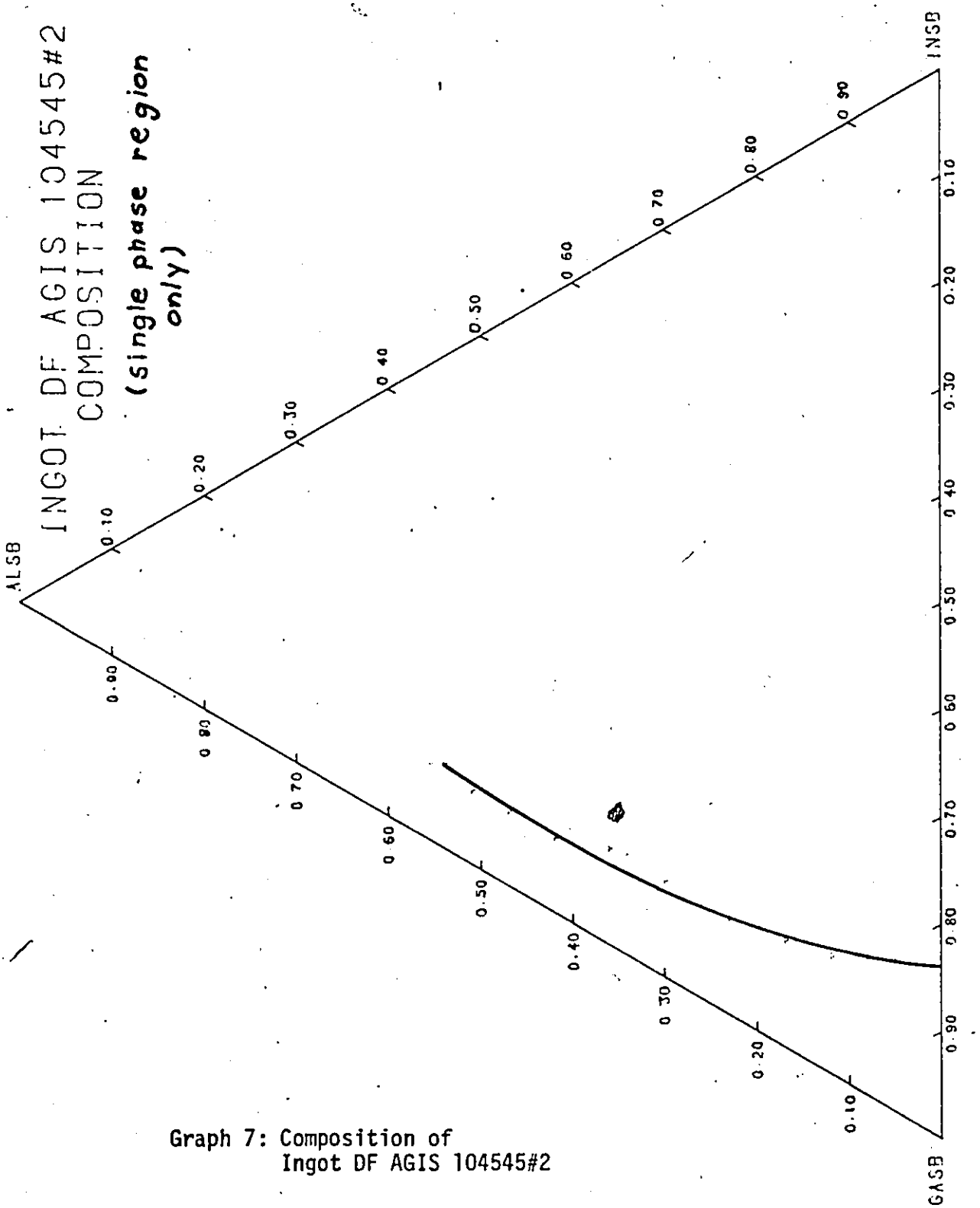

Graph 7: Composition of
Ingot DF AGIS 104545#2

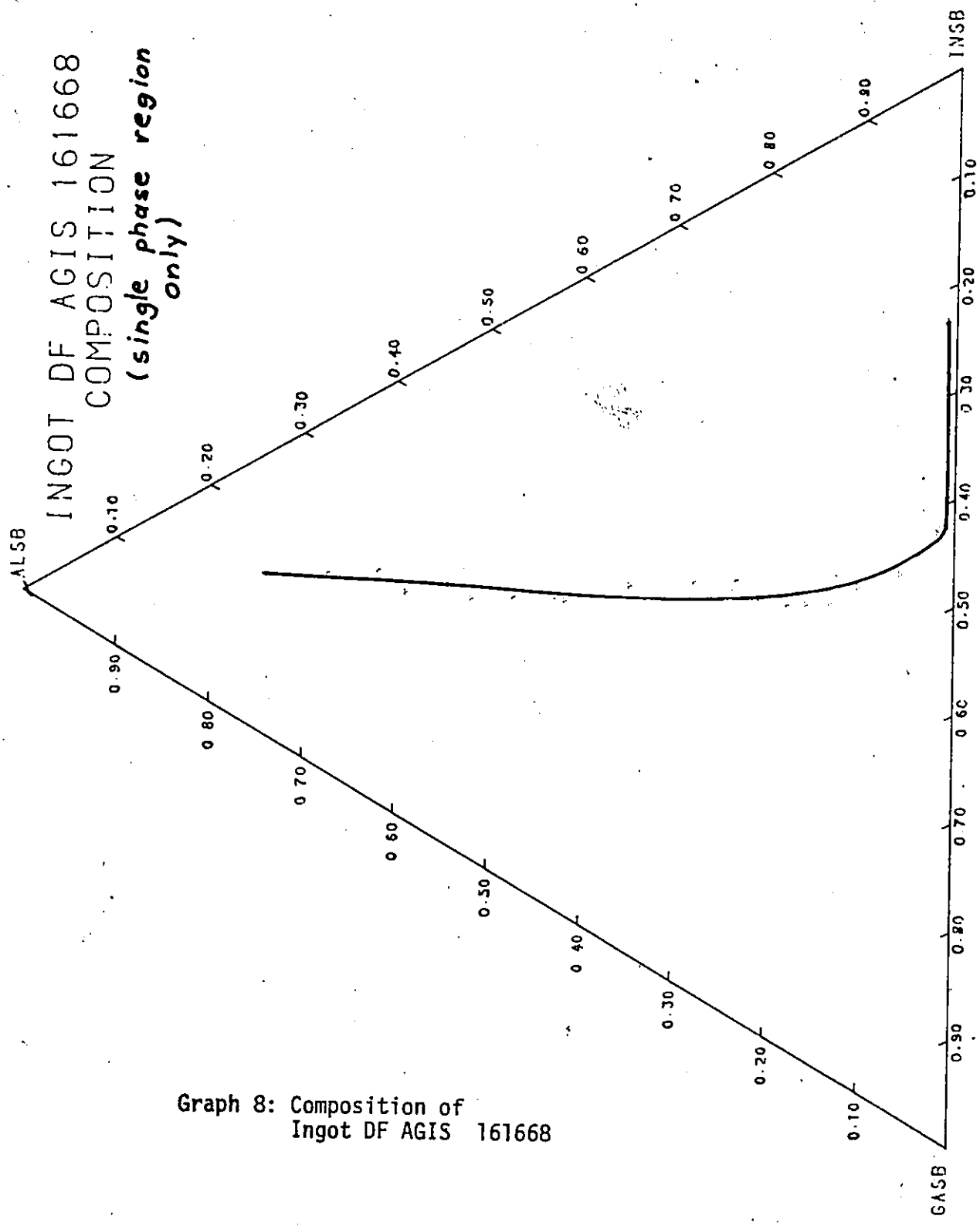

Graph 8: Composition of
Ingot DF AGIS 161668

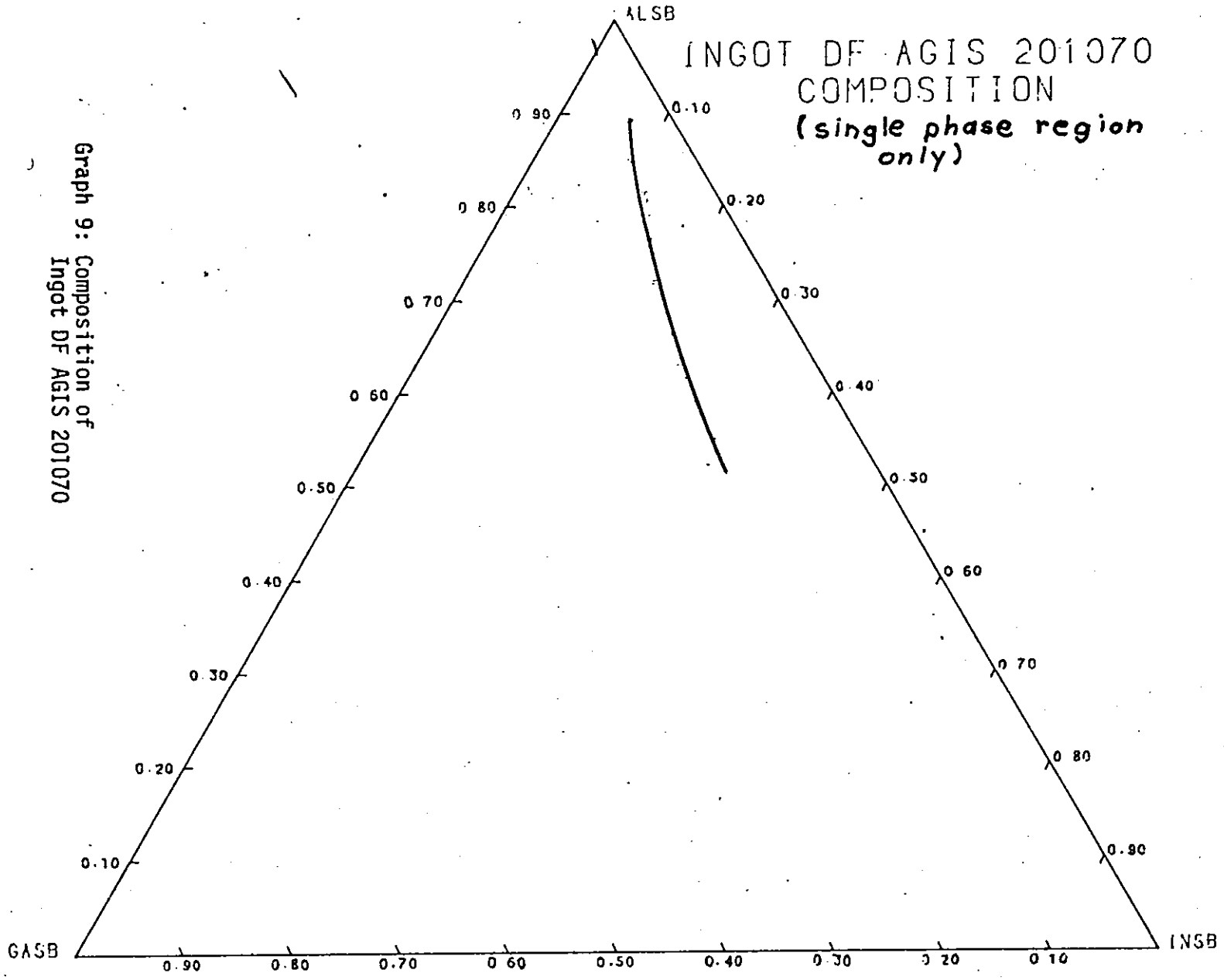

Graph 9: Composition of Ingot DF AGIS 201070

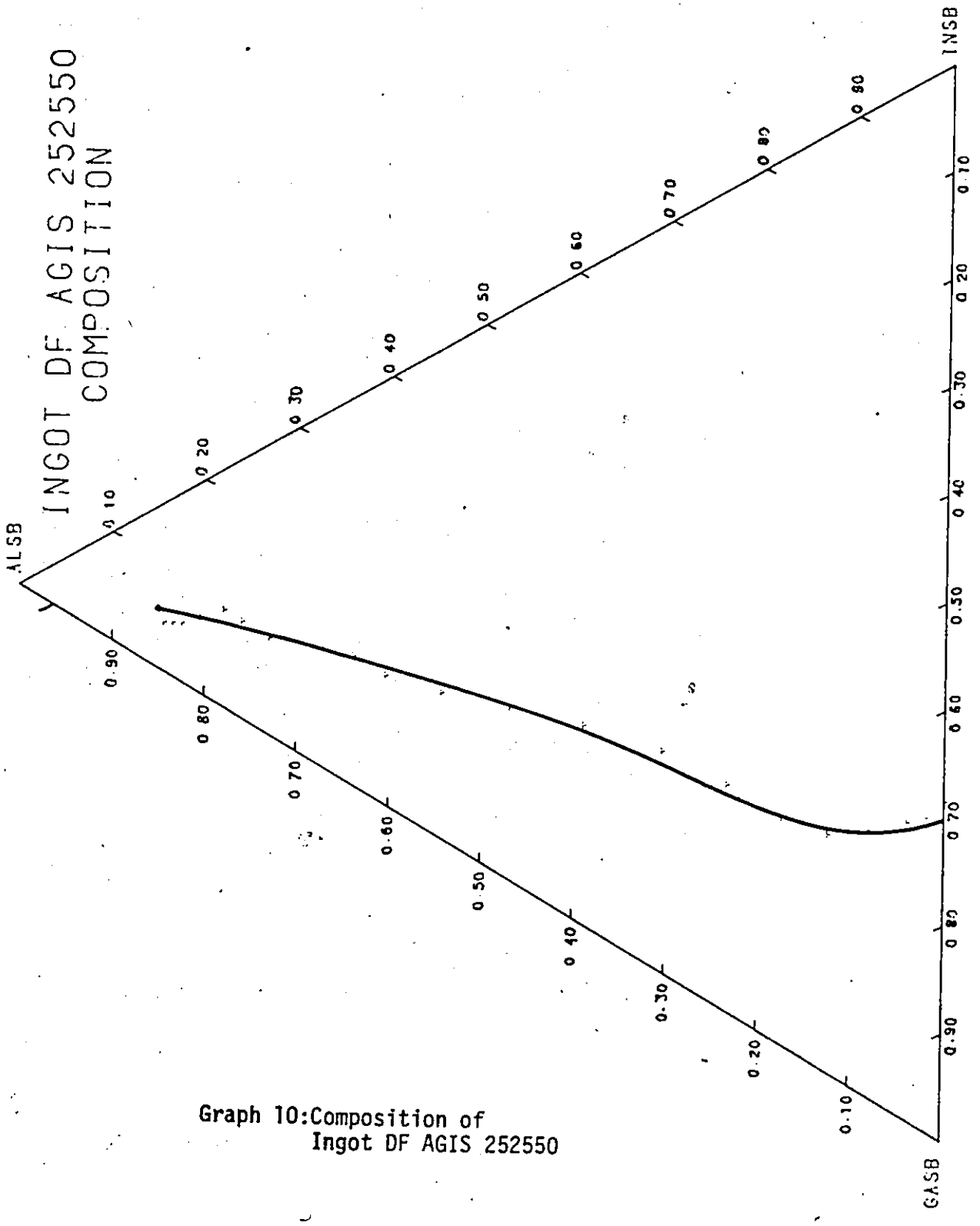

Graph 10:Composition of
Ingot DF AGIS 252550

Chapter IV

DETERMINATION OF THE LATTICE PARAMETER

If the slices were to be used, it was necessary to establish that they were single phase. This was done by a standard X-ray powder photography method using a Debye-Sherrer camera, and Cu-Kα radiation. For the X-ray analysis, a small piece was cut from the slices (such that the piece would contain material from both sides of the slice (establishing a somewhat more reliable average)). This piece could be very small, as less than 1mg of material is necessary to take a powder photograph. It is usually more convenient to take a little more, 5-10mg if possible. Once this was done, the lattice parameter a may be readily found. In powder photographs, it is sometime necessary to correct for absorption of X-rays in the sample. The lattice parameter obtained this way is called ao. All lattice parameters were found this way. The method is standard and may be found in He 51, along with other general information about the technique of X-ray powder photography.

A selection of the slices were used to establish the lattice parameter along the ingot. Not every slice was used, but, depending on the composition gradient, every second or

third slice . If the composition gradient was very steep, every slice in that region would be used, however. The selection process does not affect the results significantly, because where the composition gradient is not very steep, the lattice parameter variation from slice to slice is not very great, so it is simply not necessary to use every one. A smoothing procedure was used for this data, which was similar to the method used for the composition vs position curves. The lattice parameter data is the most accurately known. ao can usually be determined to within .001Å.

4.1 FURTHER EVIDENCE OF THE RELIABILITY OF THE COMPOSITION DATA

Among the various slices analysed using XRF, some showed nearly zero AlSb, and had their lattice parameters determined. If these compositions are accurate, then we can compare the XRF composition determination with that based on Vegard's law (linear variation of lattice parameter with x. This is known to apply to the $Ga_xIn_{1-x}Sb$ system (Wi 6d)) The results may be seen in table 6.

The agreement here is good, and is favourable evidence that the composition data is reliable. Unfortunately, no samples of $Ga_xAl_{1-x}Sb$ or $In_xAl_{1-x}Sb$ were available, so all aspects of the XRF analysis could not be tested by this method. Graphs of lattice parameter vs position follow.

TABLE 6

Comparison of compositions determined from lattice parameters with those determined from XRF

All AlSb concentrations are zero
Composition measurements are in atomic fractions

Sample	Lattice Parameter (Å)	Composition (Vegard's law)		Composition (XRF)	
		GaSb	InSb	GaSb	InSb
161668 5.6cm	6.395	.222	.780	.200	.800
6.7cm	6.426	.138	.862	.125	.875
9.4cm	6.464	.040	.960	.050	.950
201070 5.3cm	6.401	.203	.797	.210	.790
6.2cm	6.417	.160	.840	.150	.850
12.0cm	6.470	.023	.977	.025	.975
104545 1.6cm	6.147	.866	.134	.840	.160
#2 2.7cm	6.237	.630	.370	.660	.340
4.9cm	6.473	.013	.987	.010	.990
103060 1.0cm #2	6.169	.810	.190	.800	.200
252550 7.3cm	6.209	.704	.296	.685	.315

We see from these graphs (11-15) that, in general, the lattice parameter increases slowly and smoothly with distance. This is consistent with the composition measurements, which show a decreasing aluminum concentration with distance. Since the lattice parameter of AlSb is low, we would expect aluminum rich alloys to have a lower lattice parameter. Graph 12 is of interest, because it shows that, within experimental error, ingot 104545#2 followed a line of constant lattice parameter. This was useful information to know when it came to fitting the lattice parameter data. As in the graphs of composition vs distance, only the regions with a significant AlSb concentration are shown, and smooth curves are drawn only when the samples were single phase.

Graph 11: Lattice parameter vs distance
for Ingot DF AGIS 103060#2

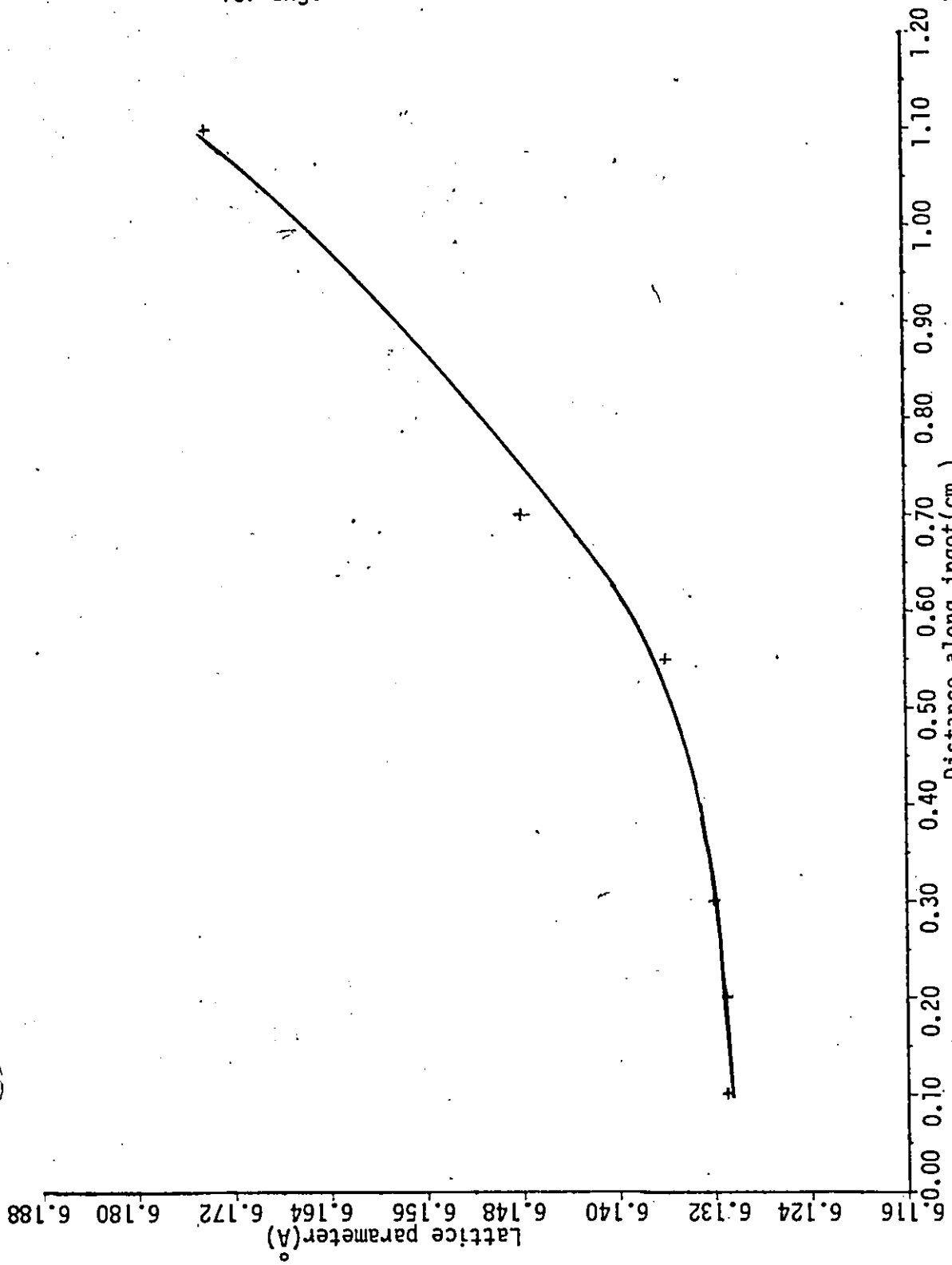

Graph 12: Lattice parameter vs distance
for Ingot DF AGIS 104545#2

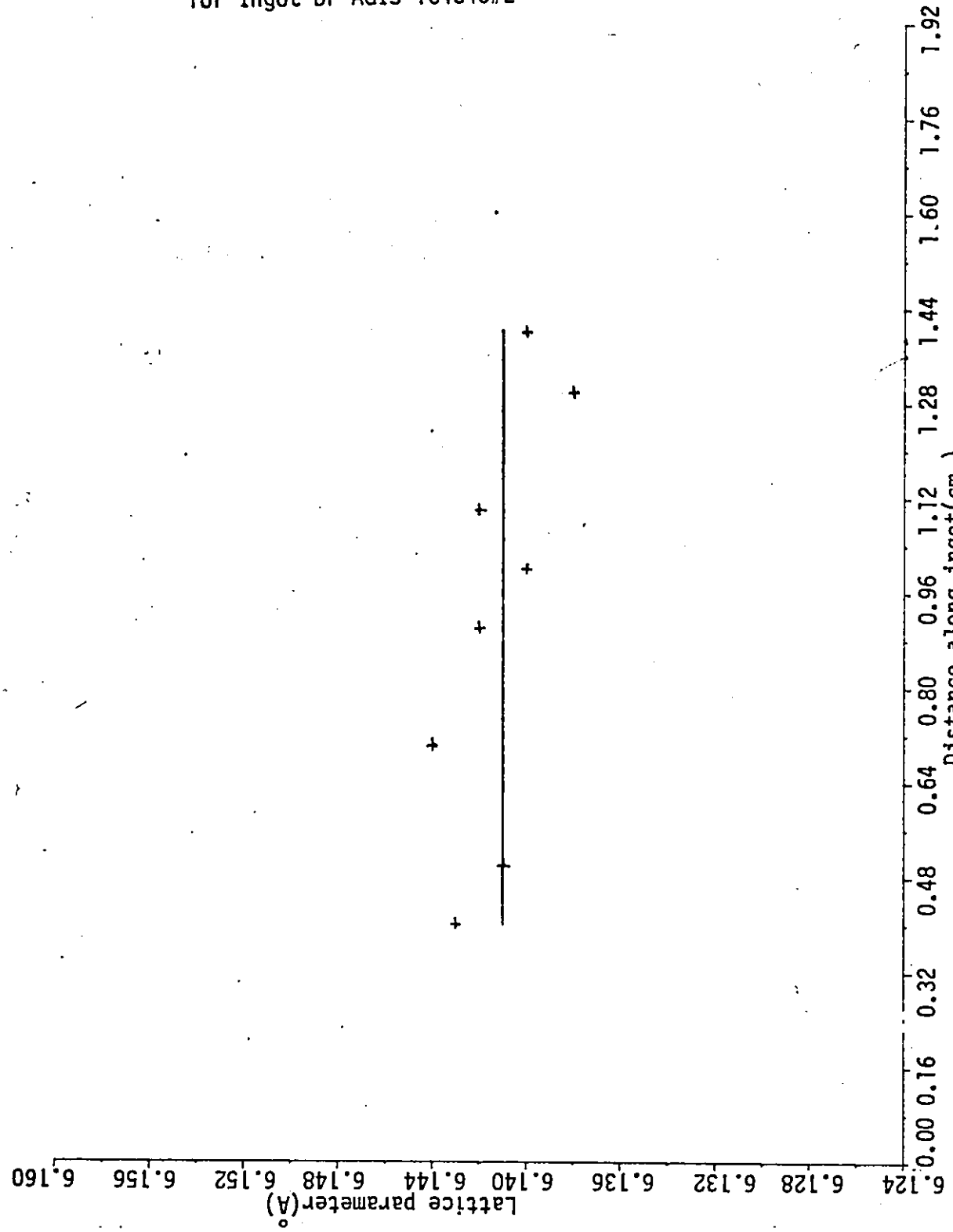

Graph 13:Lattice parameter vs distance
for Ingot DF AGIS 161668

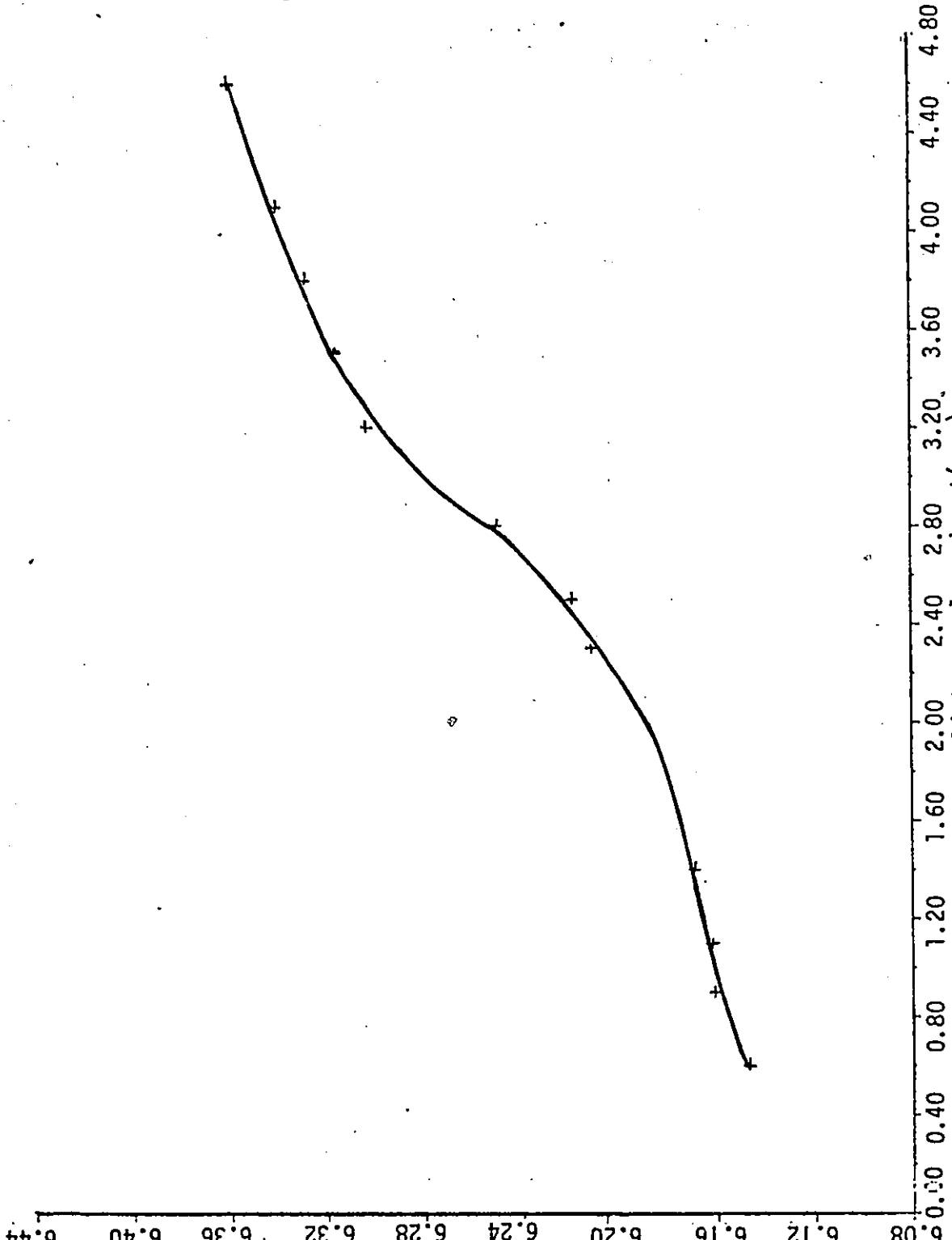

Graph 14:Lattice parameter vs distance
for Ingot DF AGIS 201070

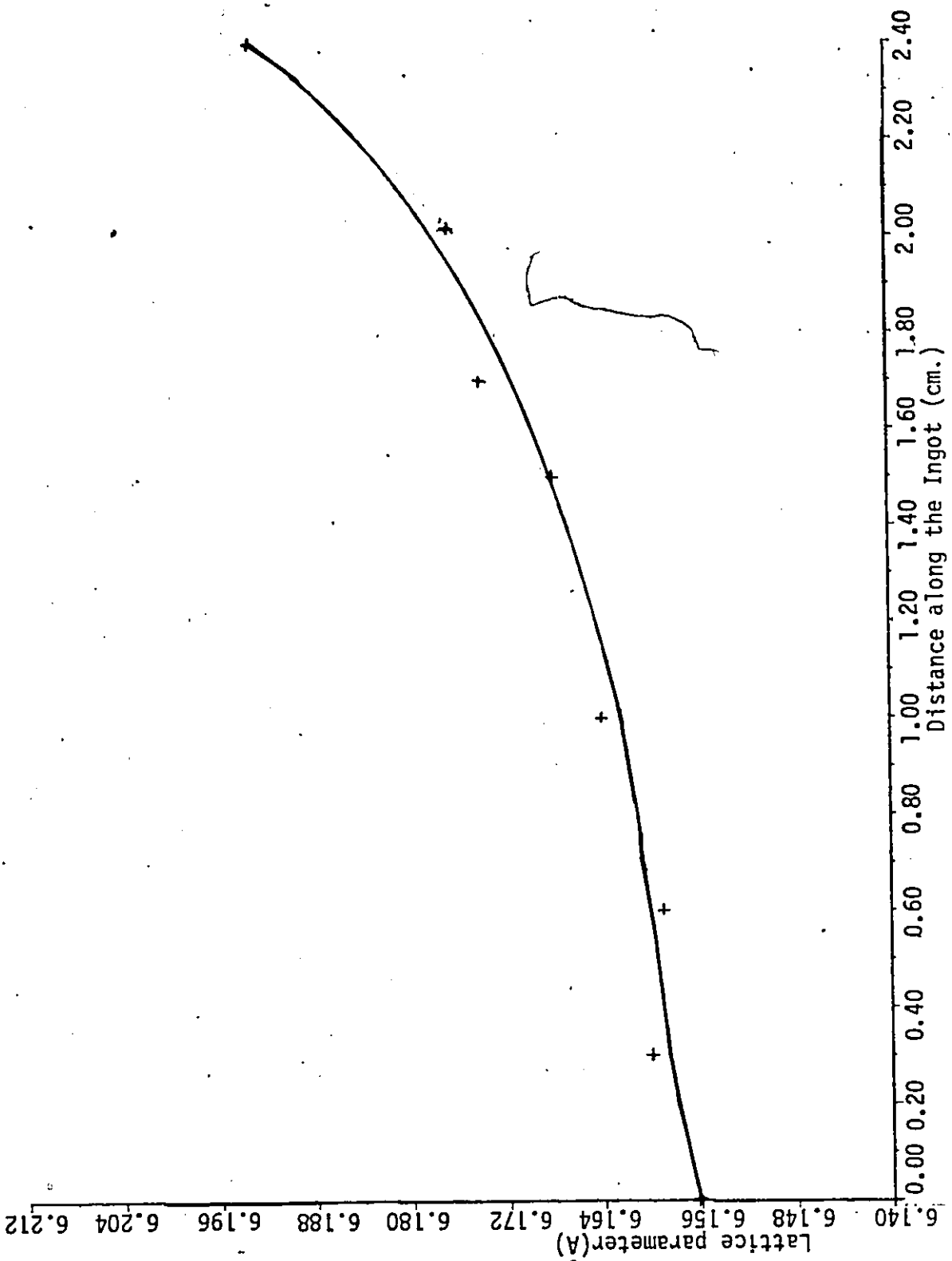

Graph 15: Lattice parameter vs distance
for Ingot DF AGIS 252550

Chapter V

ENERGY GAP DETERMINATION

Various slices from the ingots (selected on the basis of the composition gradient, as explained in the lattice parameter section), which were shown to be single phase by X-ray powder photography, were lapped by hand in a paste of 5000 mesh aluminum oxide powder and methanol (water cannot be used, as Al compounds will react with water), until they were between 90 and 180 microns thick. The thin slices were washed off afterwards, but were not otherwise polished or treated. The transmission as a function of wavelength (at room temperature) was determined for these slices. The following setup was used to make these measurements (figure 5). The preamp and selective amplifier were not used in all the measurements, but only if there was insufficient signal using the selective amplifier alone.

The theory of optical absorption is well known (see for example, Sm 59 and Ab 72), so only the relevent details will be discussed here. The minimum energy gap in the $Al_xGa_yIn_{1-x-y}Sb$ system is expected to be an allowed indirect transition in part of the range of compositions, and a direct transition for the rest. For a direct transition, the following relation is known to hold:

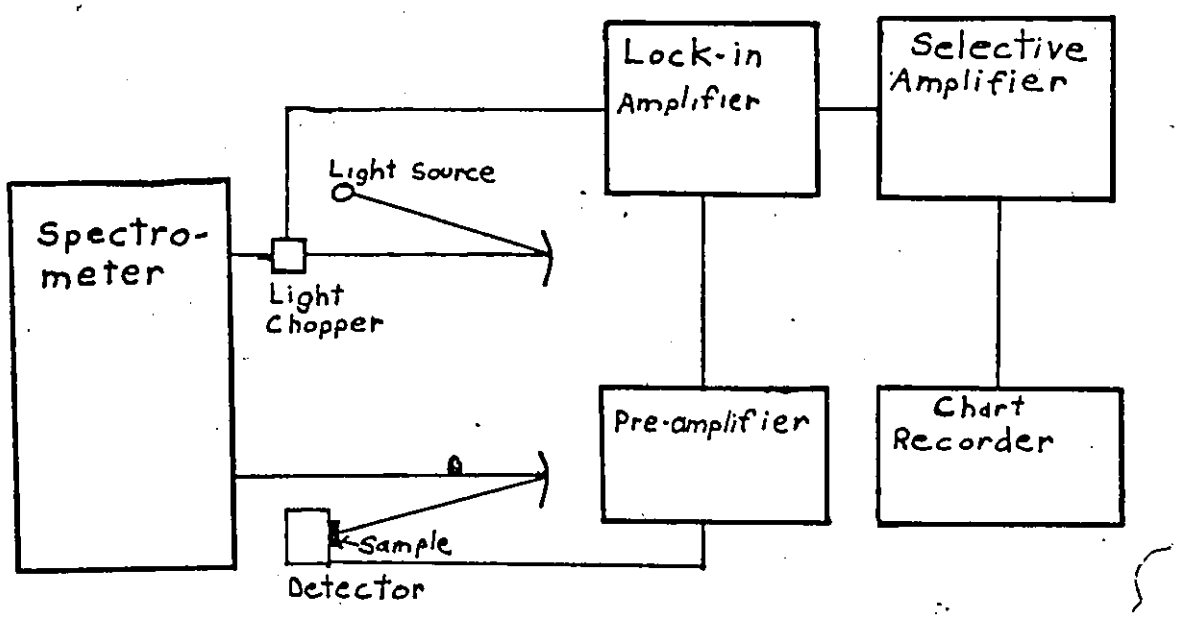

Figure 5: Apparatus used in the transmission measurements

$$|\alpha h\nu| = B(h\nu - Eg)^{1/2} \qquad (19)$$

where α is the absorption coefficient, h is Planck's constant, and ν is the frequency of the light passing through the sample. This relation is well satisfied for direct gaps, and there are no problems associated with determining Eg in the direct gap region. To find the direct gap one plots a graph of $(\alpha h\nu)$ vs $h\nu$ (α first has the background a subtracted from it, as is the usual procedure). This graph has a linear region, and if this linear region is ex-

trapolated to $\alpha=0$, the intercept should be Eg. This is the procedure that was followed. See figure 6 for some sample curves.

For an allowed indirect transition, the following relation is expected to hold:

$$|\alpha h\nu| = B(h\nu-Eg)^2 \qquad (20)$$

But it turns out that in AlSb (hence one might reasonably expect also in most of the indirect gap region of the system) this relation is not satisfied by the experimental data (Wi 66). Optical absorption measurements were made on a specimen of pure AlSb, and it was confirmed that assuming relation (20) could not give an Eg which agreed with the values commonly quoted in the literature (1.60-1.65ev, see Wi 72).

There are, however, other ways of determining the energy gap. One method which has been used is to take the energy gap as the energy where α is a certain level above the background absorption. Thomas (Th 69) has made studies of the various criterion of this sort for determining the energy gap. It turns out that by choosing the Eg to be at the point where α is 150cm^{-1} above the background a gives results which are comparable with those obtained using relation (19). (300 or 100cm^{-1} are not bad either). If we use

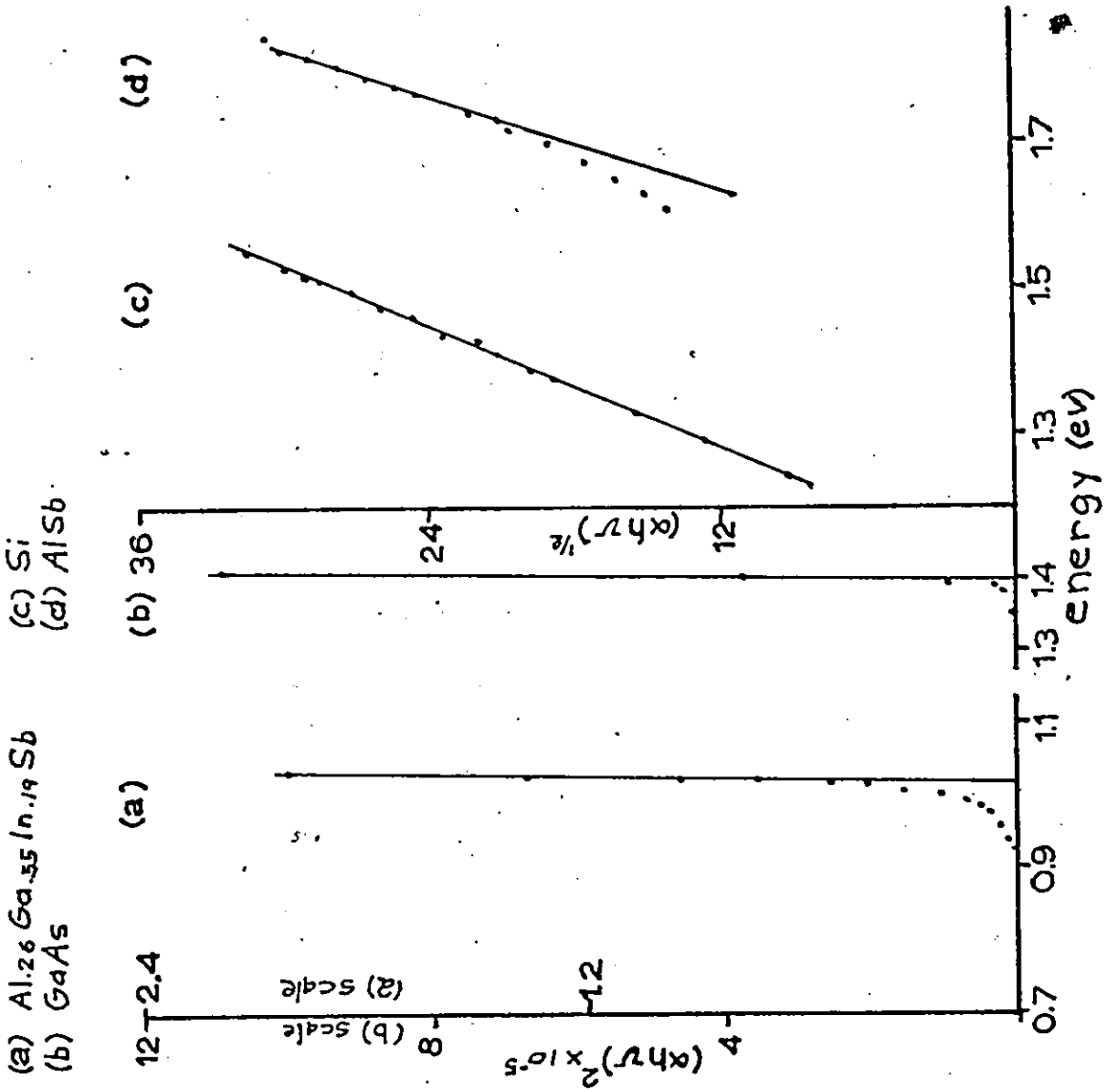

Figure 6: Some typical absorption curves

Results for GaAs (known to be a direct gap material) and Si (known to have an indirect minimum energy gap) are shown for comparison. Notice that the curve for AlSb is very much unlike that for silicon, thus confirming that the behaviour is not as would be expected. Figure 6a shows a curve for a typical material in the middle of the composition triangle (direct gap). These curves typically fall more slowly with decreasing energy than in the case of GaAs, since the materials do have a small composition gradient.

the 150cm-1 criterion as a basis for establishing the energy

gap then we obtain an Eg for AlSb which agrees with those obtained by others. For this reason it was decided to use this method as a basis for determing the values of Eg. Curves of Eg vs position along the ingot were constructed, and smooth curves were drawn through the points, using the same ideas as were used in the smoothing procedure for the compositon curves. These curves follow. As expected, since the AlSb concentrations are dropping with distance, so does the energy gap, since AlSb has the highest energy gap of the three antimonides. The graphs(16-20) do not exhibit any unusual behaviour when the minimum energy gap becomes direct. As in the composition and lattice parameter vs distance curves, only the single phase regions with a significant AlSb concentration are shown on the graphs. It may be seen that there is a degree of scatter among the points, so that the choice of the method of Eg determination is not that critical. In addition for these graphs, it should be noted that due to limitations of the equipment, no measurements of energy gaps below about 0.4ev were possible, so there were a few single phase samples with a positive AlSb concentration that did not have their energy gaps determined. It is hoped that these samples will be measured sometime in the future. As a further check on the data, the following samples had the Eg determined, and also had approximately zero AlSb, so we can compare the composition determined using XRF with that based on the energy gap.

TABLE 7

Comparison of compositions determined from absorption measurements with those determined by XRF					
Composition measurements are in atomic fractions All AlSb concentrations are zero					
Sample	Energy gap(ev)	Composition (absorption)		Composition (XRF)	
		GaSb	InSb	GaSb	InSb
252550 7.3cm	.48	.685	.280	.720	.280
104545 1.6cm #2	.55 (est.)	.840	.160	.810	.190
103060 1.0cm #2	.52 (est.)	.800	.200	.780	.220

Graph 16:Energy gap vs distance for
Ingot DF AGIS 103060#2

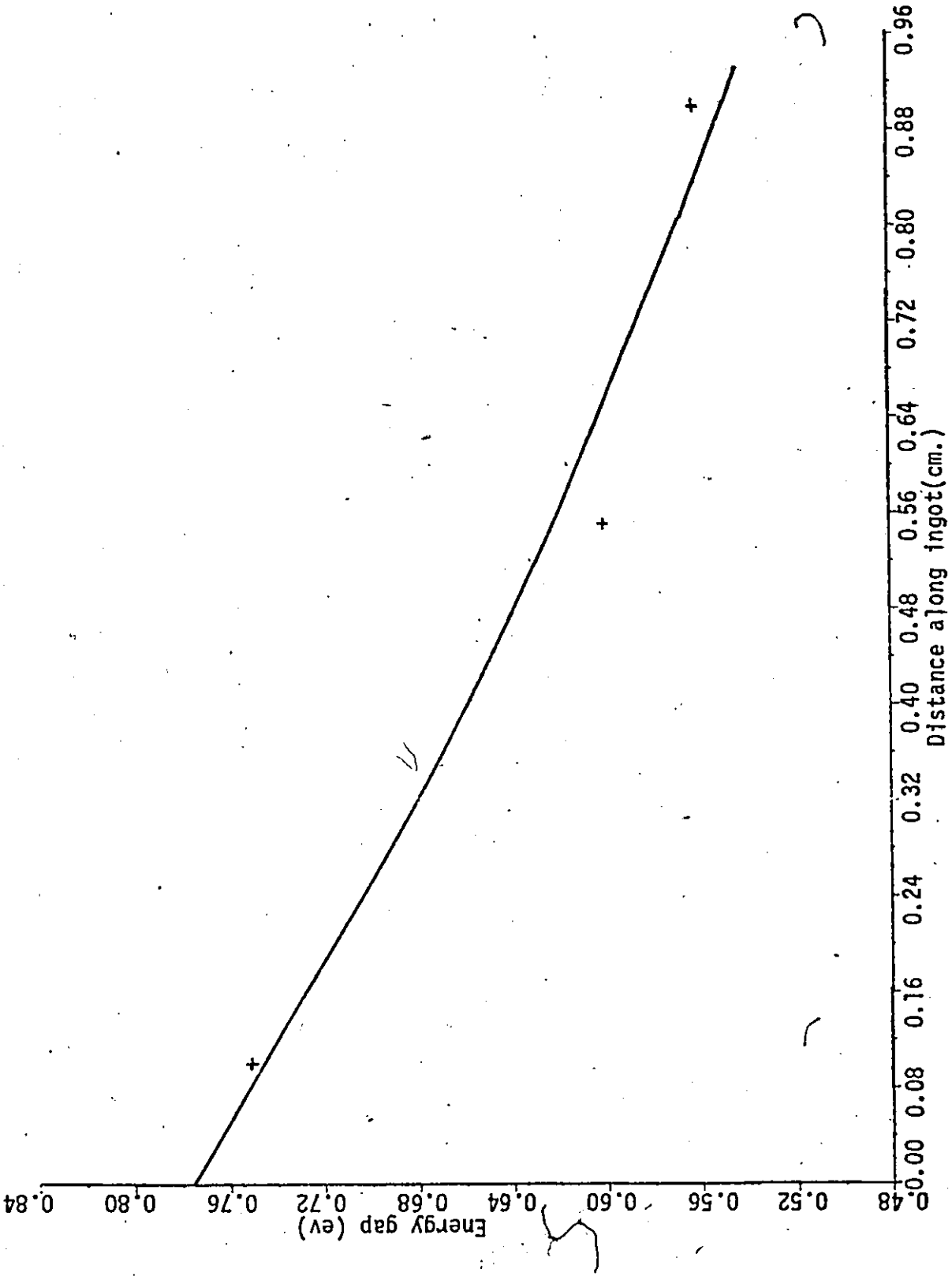

Graph 17: Energy gap vs position for
Ingot DF AGIS 104545#2

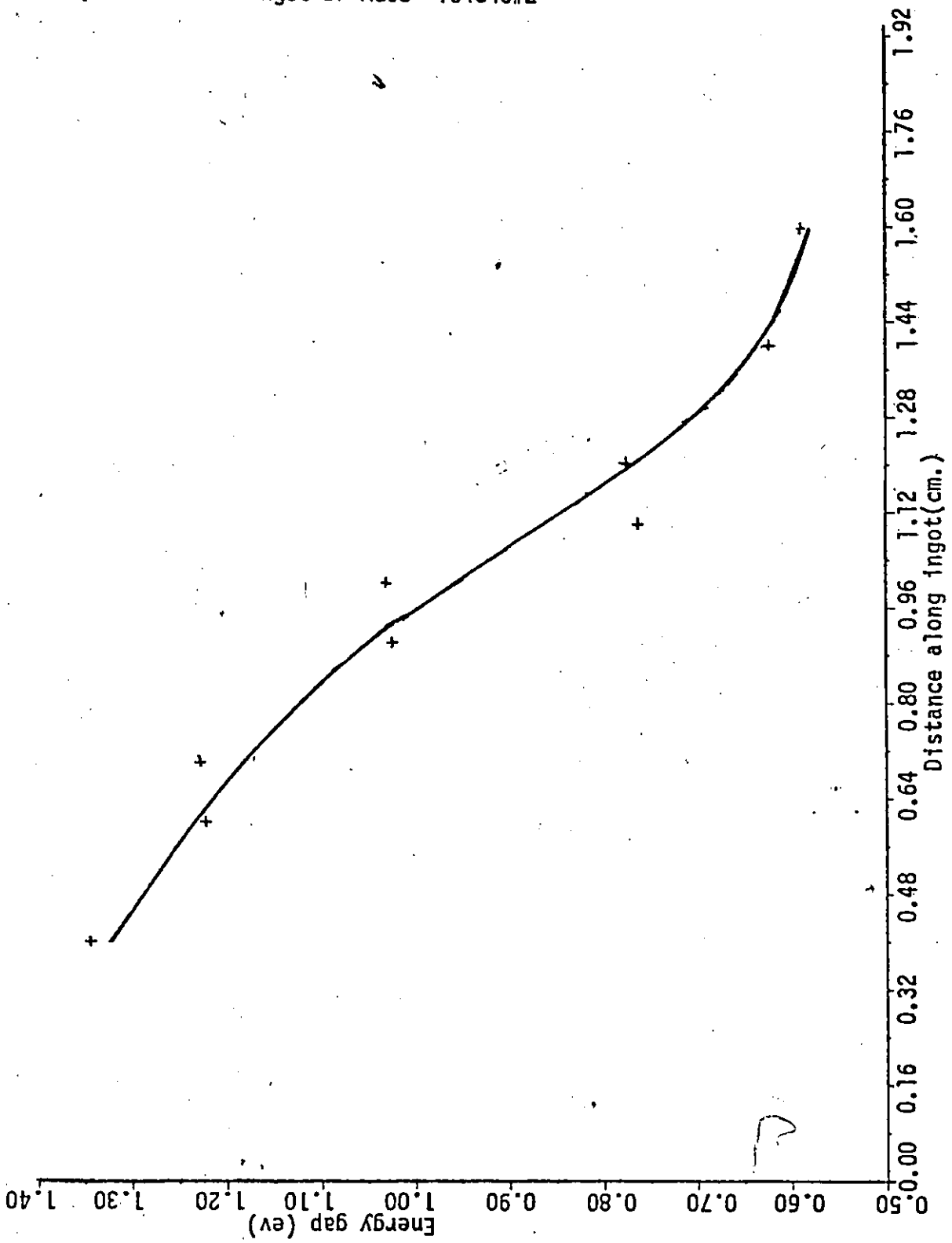

Graph 18: Energy gap vs distance for
Ingot DF AGIS 161668

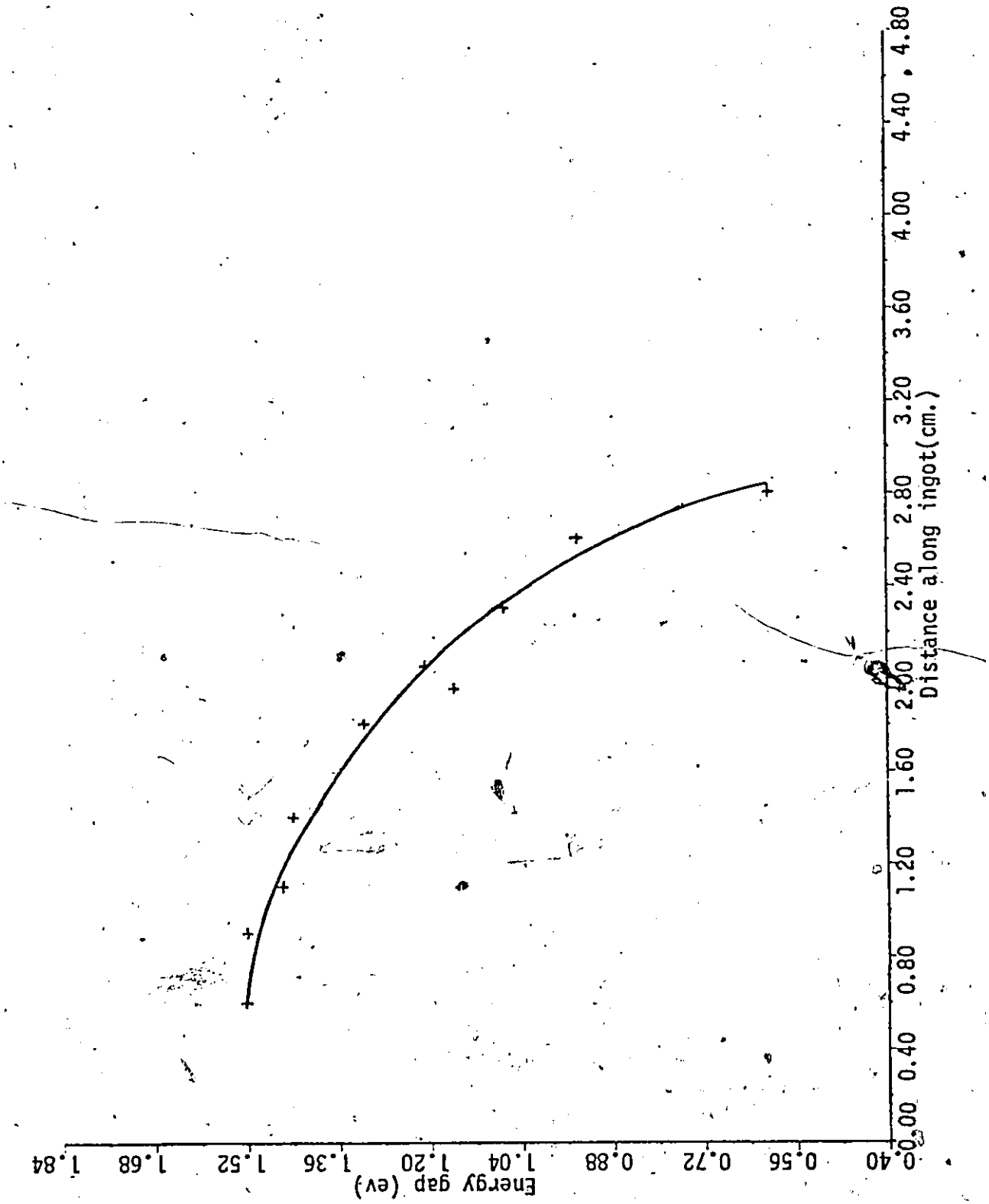

Graph 19: Energy gap vs distance for
Ingot DF AGIS 201070

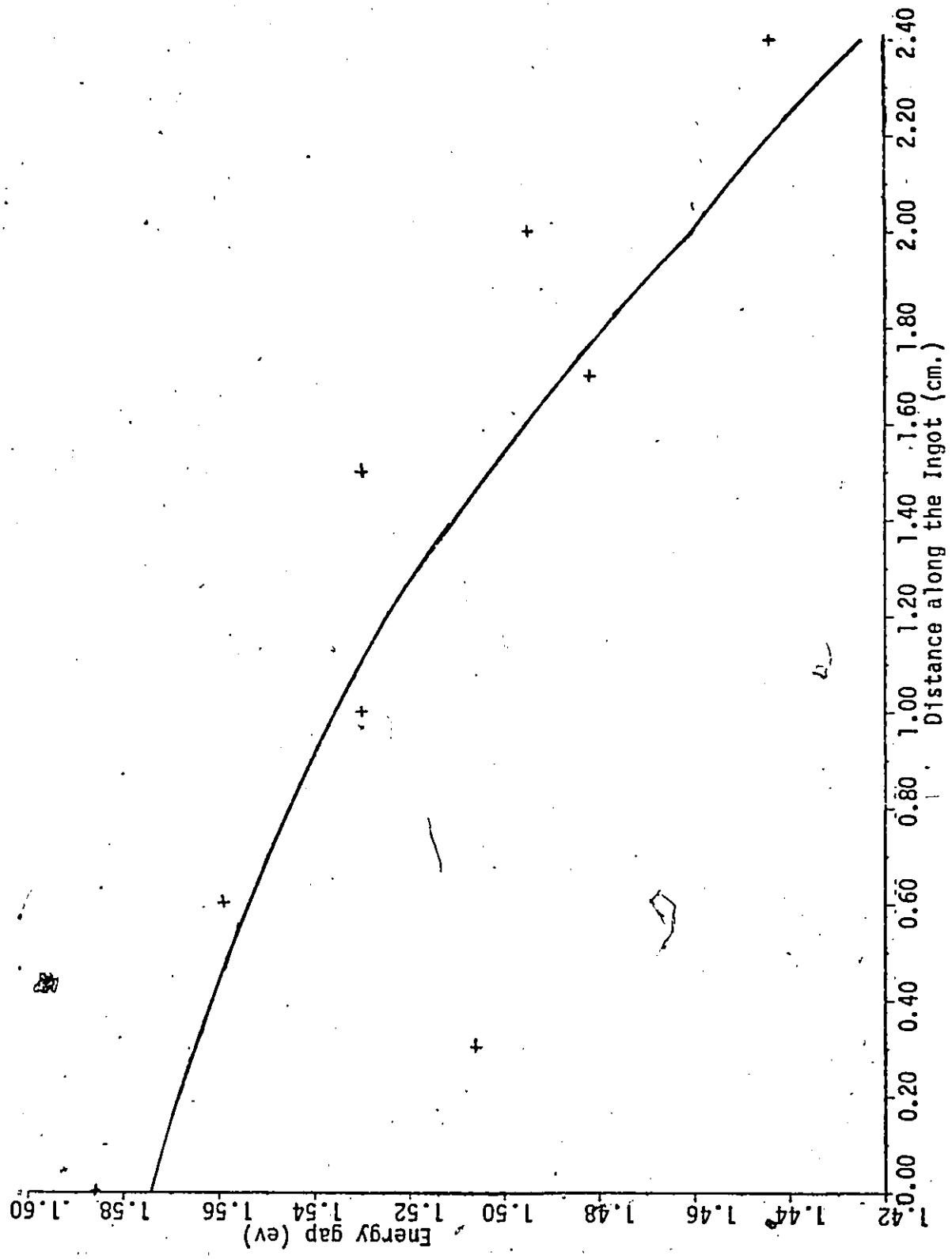

Graph 20: Energy gap vs distance for
Ingot DF AGIS 252550

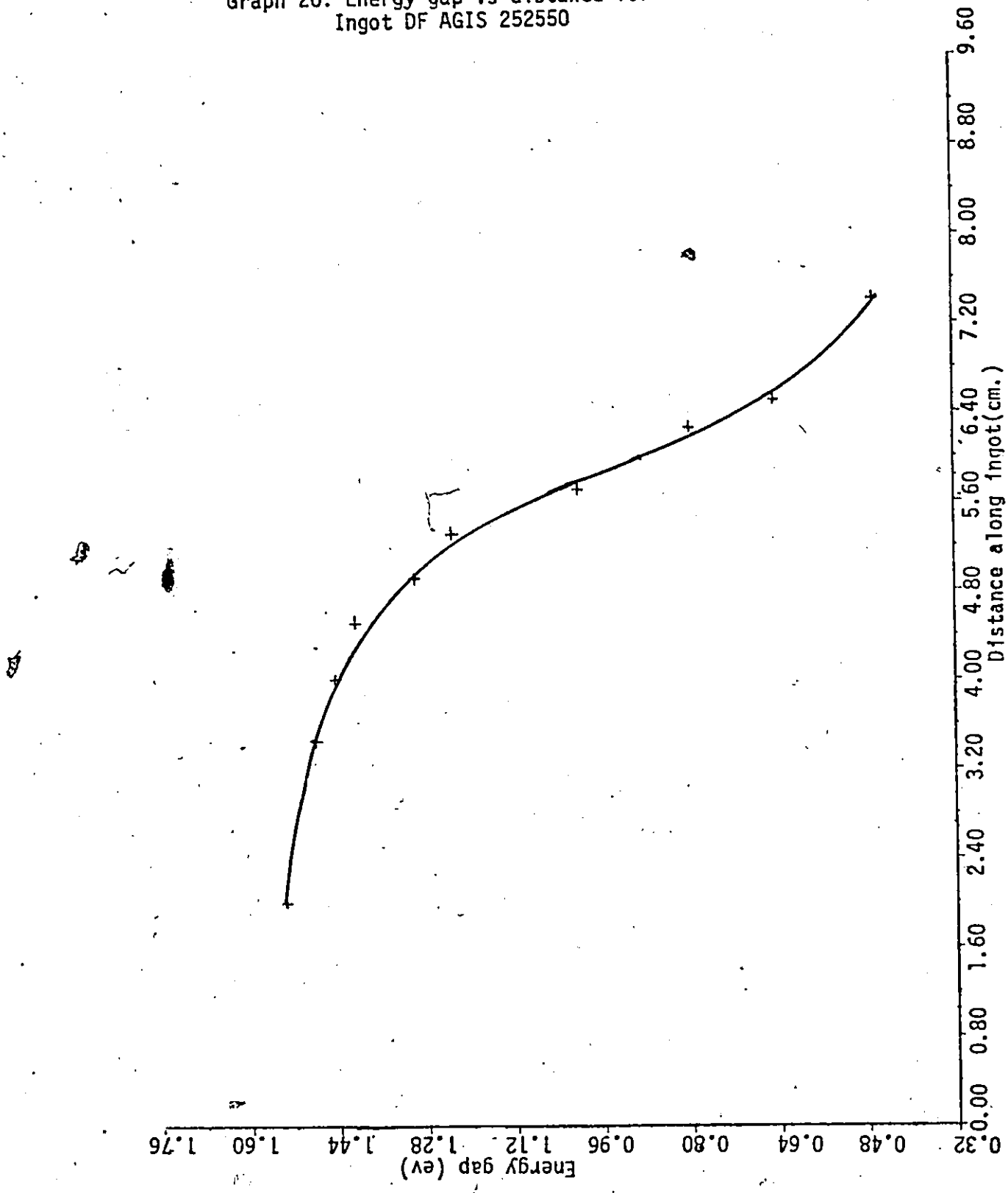

Chapter VI

FITTING THE DATA

6.1 INTRODUCTION

Since the main purpose of this work is to characterize the $Al_xGa_yIn_{1-x-y}Sb$ system, in order that the composition may be determined without recourse to XRF or electron microprobe techniques, it would be valuable if a set of equations could be obtained which would fit the lattice parameter and energy gap data as a function of composition. This was attempted, and it is believed that it has been reasonably successful.

6.2 FITTING THE LATTICE PARAMETER DATA

It is assumed that the sides of the composition triangle are known, and follow Vegard's law. This is a good approximation for these alloy systems (Wi 66). If the only requirement is that the equation satisfies Vegard's law on the sides of the composition triangle then the equation is:

$$av = 6.4789 - 0.3433x - 0.3834y \ (\text{Å}) \qquad (21)$$

(data taken from We 70). If this is the true equation, then $a_0 = av$. However, this is not true, so we must add additional terms. Since av fits the sides of the composition

triangle, the only non-vanishing terms must be in xyz (z=1-x-y). The simplest general form of the equation with additional terms is

$$ao = av + xyz(A+Bx+Cy) \qquad (22)$$

therefore

$$\frac{ao-av}{xyz} = A+Bx+Cy$$

and the coefficients may be obtained by standard fitting methods. If the equation is even simpler, of the form

$$\frac{ao-av}{xyz} = A+ B(x, y, \text{or } z) \qquad (23)$$

then the coefficients can be obtained graphically. A reasonable fit was obtained with A+Bz, where A=-0.25 and B=-3.25. So the complete equation is:

$$ao = 6.4789-0.3433x-0.3834y + xyz(-0.25-3.25z) \quad (\text{Å}) \qquad (24)$$

69 points were used in the fitting procedure, and the standard deviation σ =.010Å corresponds to a few % in composition. The contours of this equation plotted on triangular coordinate paper, along with all the data points, appear at the end of this chapter.

6.3 FITTING THE EG DATA

Since part of the range of compositions has an indirect gap, and part has a direct gap, each part had to be fitted separately. To do this one had to estimate where the indirect gap region was, since it was not known. It was, however, generally obvious whether a point was better fitted in the direct or indirect gap region.

The direct gap is known along the edges of the composition triangle, and this information was used in the fitting procedure. The indirect gap is known for the $Ga_xAl_{1-x}Sb$ edge. It is also known for AlSb and at the point on the $In_xAl_{1-x}Sb$ system where the direct and indirect gaps are equal($x=.4$), but otherwise it is not well known. It was assumed to be linear along this edge. This is probably a reasonable approximation, at least for the upper ($x<.5$) region of the $In_xAl_{1-x}Sb$ system(personal communication, J.C.Woolley). For the $Ga_xIn_{1-x}Sb$ system, the indirect gap is not well known, so once again it was decided to assume that it was linear, based on the known value for GaSb and the extrapolated value for InSb. The fact that these values are not well known is not very important, because these values are used only to make the fitting procedure easier. A fit is desired only in the region far from these unknown edges. No attempt is made to claim that the fit is reliable near these unknown edges.

6.3.1 Direct gap

If we take the known fits to the edges of the composition triangle, then we can obtain the following equation, which fits the edges only:

$$Epd = 0.095 + 1.76x + 0.28y + 0.345(x^2 + y^2) + 0.085z^2 \quad (ev) \qquad (25)$$

TABLE 8

Summary of data and sources used in fitting the energy gap data

(values are in ev)

Direct gap

System	Equation	Source
$Ga_xIn_{1-x}Sb$	Ed= 0.18 + 0.11x + 0.43x	Th 67
$Ga_xAl_{1-x}Sb$	Ed= 0.72 + 0.79x + 0.69x	Au 75
$Al_xIn_{1-x}Sb$	Ed= 1.02 + .085x + .525x	Is 74

Indirect gap

System	Equation	Source
$Ga_xAl_{1-x}Sb$	Ei= 1.02 + .085x + .525x (modified so that Ei=1.63 when x=1)	Au 75
$In_xAl_{1-x}Sb$	Ei=.805 + .825 (estimated from known value when x=.4 (1.30) from Ag 72, and an average value from various sources of 1.63 for x=1)	estimated
$Ga_xIn_{1-x}Sb$	Ei= 0.805 + 0.215x	estimated

Thus, any additional terms must contain xyz. The simplest general form of this solution is

$$Egd = Epd + xyz(A + Bx + Cy) \tag{26}$$

where Egd is the direct energy gap. A similar fitting procedure was used in this case as was done for the lattice parameter case. A reasonable fit was obtained with

$$Egd = Epd + xyz(23-28y) \tag{27}$$

27 points were used in this analysis, and a standard deviation of σ=.03ev was obtained.

6.3.2 Indirect gap

A similar procedure was used for the indirect gap. The parabolic fit is:

$$Epi = 1.0675 + 0.30x - 0.31y + 0.2625(x^2 + y^2 + z^2) \quad (ev) \qquad (28)$$

and a good fit was obtained with:

$$Egi = Epi + xyz(-5.9 + 20x) \qquad (29)$$

35 data points were used and a standard deviation of σ=.02ev was obtained.

6.4 SUMMARY

The final equations for the direct and indirect gap fit are as follows:

Direct gap:

$$Egd = 0.095 + 1.76x + 0.28y + 0.345(x + y) + 0.085z + xyz(23-28y) \quad (ev) \qquad (30)$$

Indirect gap:

$$Egi = 1.0675 + 0.30x - 0.31y + 0.2625(x + y + z) + xyz(-5.9 + 20x) \quad (ev) \qquad (31)$$

The contours resulting from these equations, as well as the actual points, may be seen at the end of this chapter.

6.5 NOTES ABOUT THE FITS

1. The points used were obtained by associating a position on the smoothed lattice parameter or energy gap vs position curve with the same position on the smoothed composition vs position curve. In others words, for a given position along the ingot, a smoothed compostion was associated with a smoothed lattice parameter or energy gap, although there may not actually have been a slice at that particular position. However, approximately the same number of points were used as there were actual slices.

2. It is not claimed that the derived coefficients have any theoretical basis. This is a purely empirical fit.

3. The contours shown here bear no resemblance to the contours based on the theoretical analysis in Gl 78 and Wi 78.

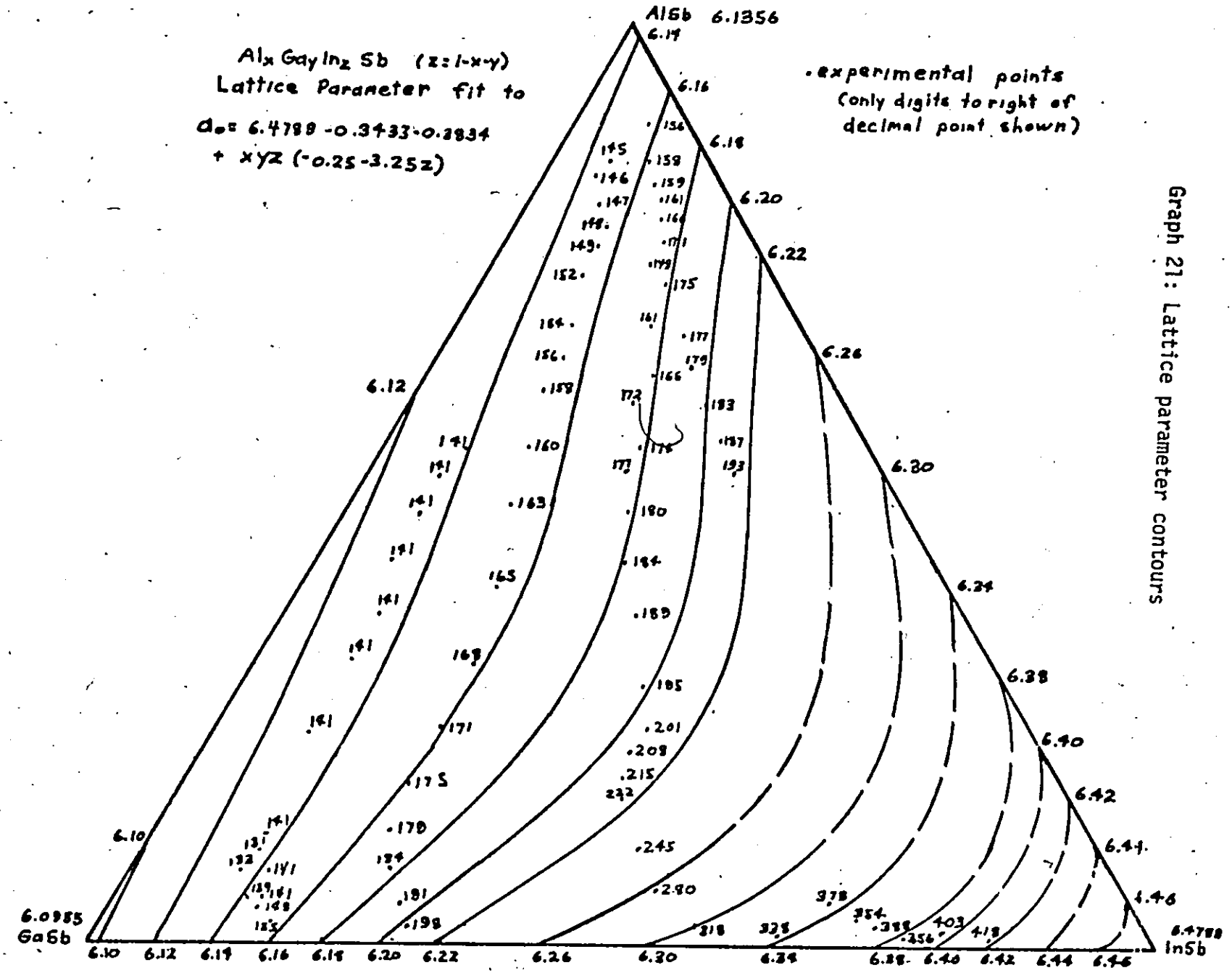

Graph 21: Lattice parameter contours

Graph 22: direct gap contours

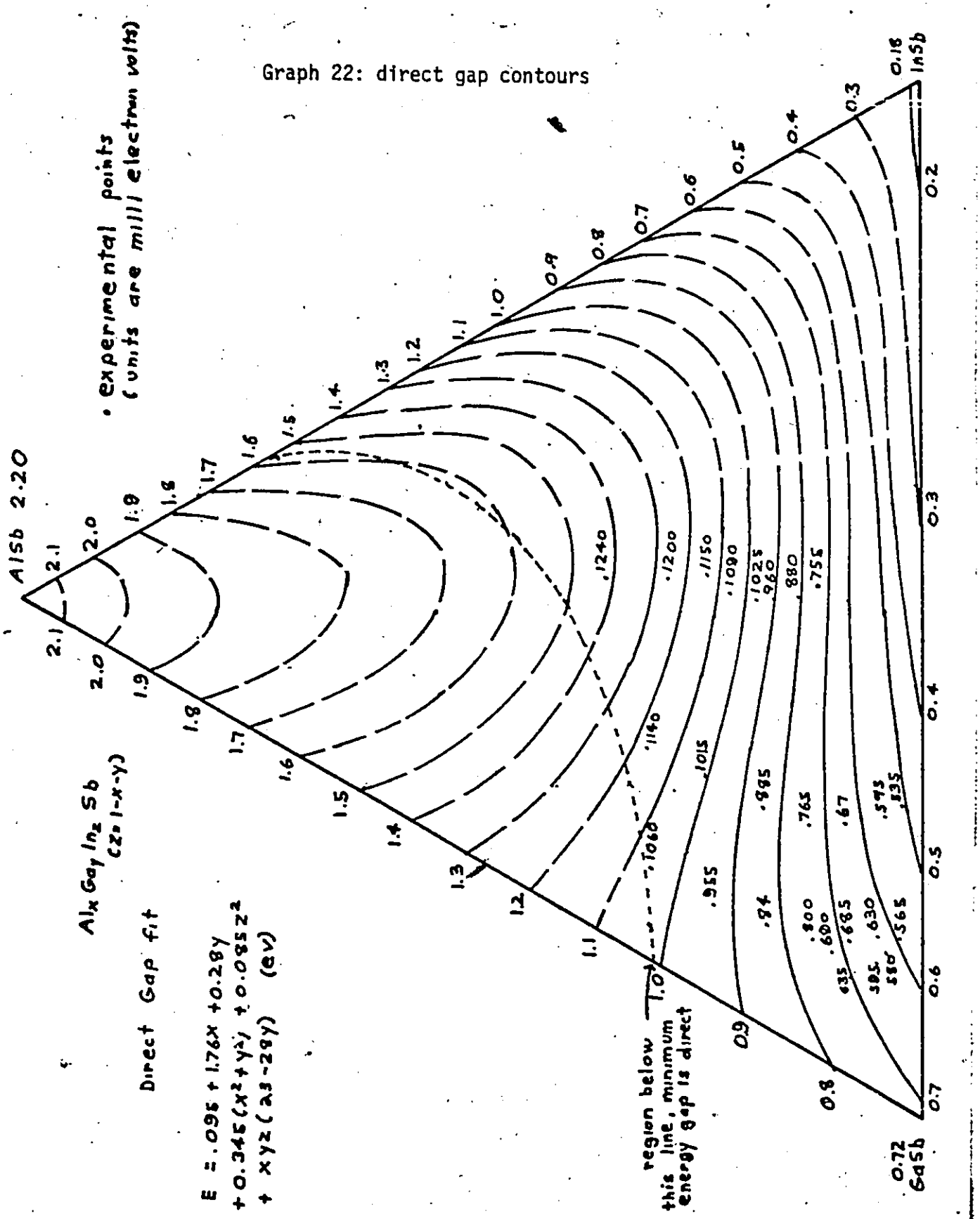

Graph 23: Indirect gap contours

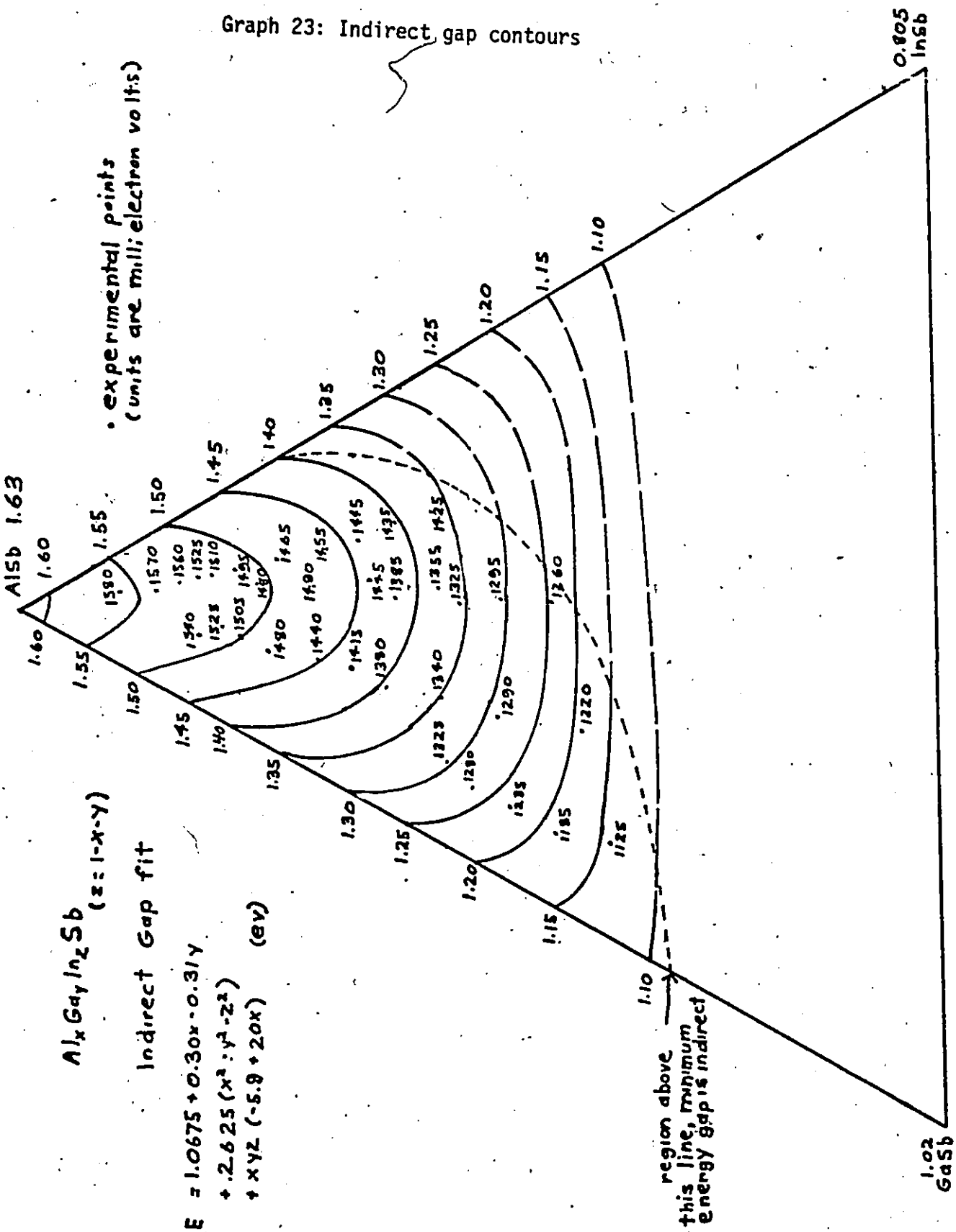

Chapter VII

THERMODYNAMIC DATA

In addition to the composition, lattice parameter and energy gap data, some other information was obtainable from this work. It was possible to establish for each successful ingot a tie line. The tie line shows the solid composition in equilibrium with a liquid of a certain composition. It was possible to determine such lines because the ingot was entirely liquid at the start, and began to freeze from one end. Since the amount frozen out at the very tip of the ingot is only a small fraction of the total ingot, the average composition of the the remaining liquid has not changed much during the freezing process. Since we know the starting composition of the ingot, and if we find the composition of the tip, then we have enough information to determine the tie line. Some of the tie lines are only estimations, since the tip was multiphase. All the tie lines are shown in the following diagram. Tie lines are useful to know because they enable the phase diagram to be determined, if the temperature at which the liquid begins to freeze is also known. Many more tie lines would be required to determine the phase diagram to any degree of completeness.

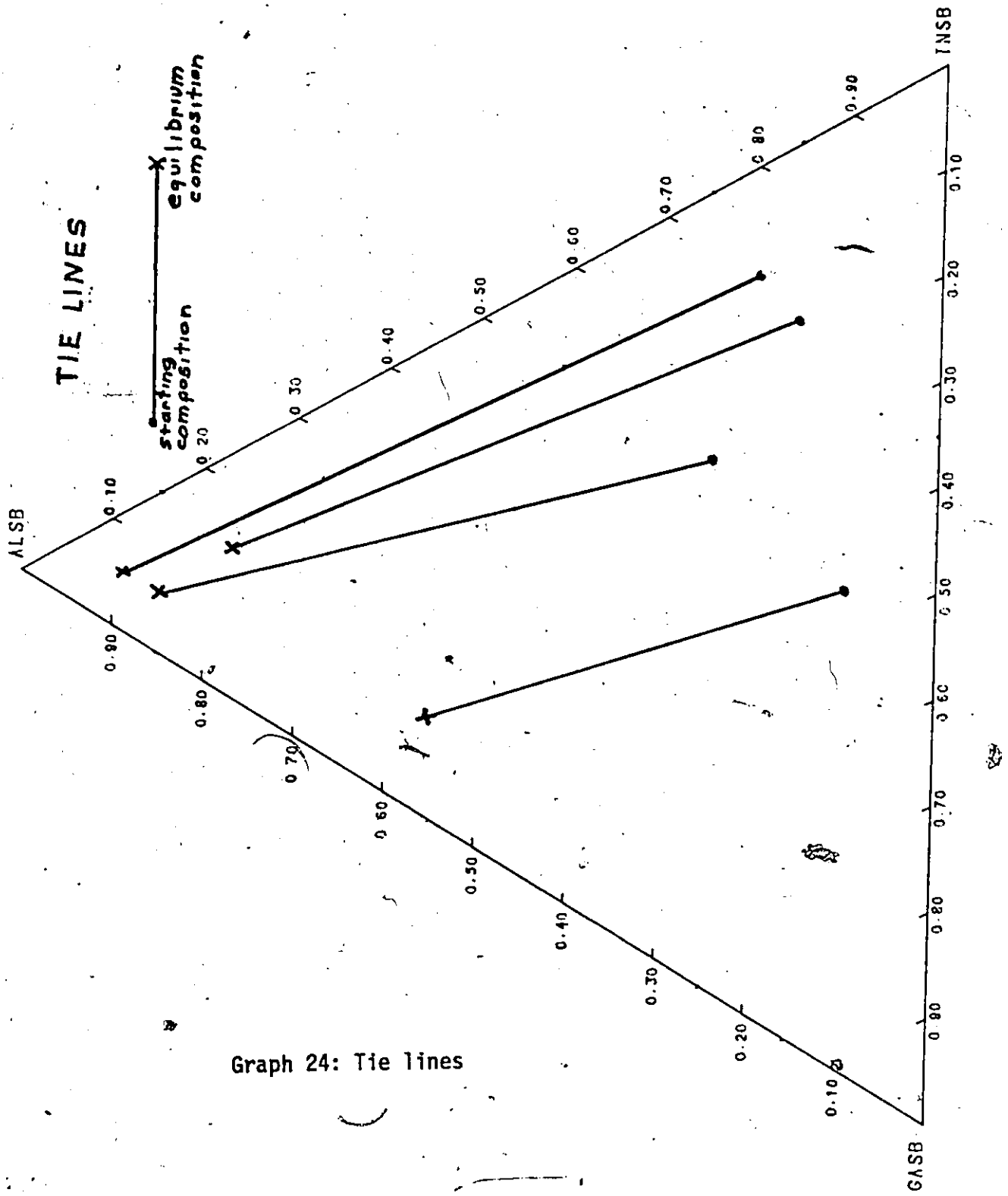

Graph 24: Tie lines

Chapter VIII

CONCLUSIONS

The quaternary III-V semiconducting alloy system $Al_xGa_yIn_{1-x-y}Sb$ was studied here. It was decided that there was a reasonable basis for supposing that complete solid solution existed in this alloy system. Existence of single phase material over most of the alloy system was later confirmed experimentally. Attempts were made to prepare single phase material by two methods:

directional freezing and annealing of pressed powders. Ingots of single phase material were successfully grown by directional freezing, but annealing for three months failed to produce single phase material.

To determine the composition of the samples, an XRF method was used. This involved the use of an X-ray spectrometer. A method of interpreting XRF data, developed by Lachance, which involves the use of α coefficients, was used. This method works reasonably well for this alloy system.

X-ray powder diffraction photographs were taken of the samples to determine if they were single phase. If this

were the case, the lattice parameter was measured, and then optical absorption measurements were made on the samples, and the minimum energy gap was determined.

Using the collected lattice parameter and energy gap data, attempts were made to find empirical equations which related this data to the composition data.

It is possible to find an equation which satisfies the known values of these quantities on the edges of the composition triangle (that is, satisfy the conditions that either AlSb, GaSb, or InSb is not present). Using only two additional parameters, determined experimentally, equations were found which fitted fairly well the data in the entire alloy system. The system is fairly well characterized by these equations. Measurements of lattice parameter and energy gap of an unknown sample should be sufficient to fix the composition to within a few % of the components. The final equations are:

The equation for the lattice parameter is:

$$ao = 6.4789 - 0.3433x - 0.3834y + xyz(-0.25 - 3.25z) \quad (Å)$$

The equation for the direct gap is:

$$Egd = 0.095 + 1.76x + 0.28y + 0.345(x^2 + y^2) + 0.085z^2 + xyz(23 - 28y) \quad (ev)$$

The equation for the indirect gap is:

$$Egi = 1.0675 + 0.30x - 0.31y + 0.2625(x^2 + y^2 + z^2) + xyz(-5.9 + 20x) \quad (ev)$$

8.1 SUGGESTIONS FOR FUTURE WORK

There is a small region in the alloy system where single phase material was not obtained. Several ingots which would have produced such material were multiphase in the desired region. This suggests the possibility that single phase material does not exist in this region. Future work will confirm or deny this.

Studies of the direct gap in the AlSb rich region of the alloy system were not possible using optical absorption, but are possible using electroreflectance. These studies would determine whether the direct gap equation has any validity in this region (note that it is not claimed to be). Currently, work is being done in this direction.

Eventually, all possible III-V quaternary systems (there are 13 of them) could be studied, as thoroughly as the ternary systems have been done.

REFERENCES

Ab 72 Abeles, ed., Optical properties of solids, North Holland publishing company, Amsterdam, 1972.

Ag 72 Ya. Agaev and N.G. Bekmedova, Soviet Phys. Semicond., 5, 1330 (1972).

Au 75 D.Auvergne et al, Solid State Communications, 17, 511 (1975).

Bi 69 L.S. Birks, X-ray Spectrochemical analysis, Interscience Publishers, New York, 1969.

Ca 66 K.G. Carr-Brion, The analyst, 91, 289 (1966).

Gl 78 T.H. Glisson et al, Journal of electronic materials, 7, 1 (1978).

Gr 78 M.F. Gratton, Ph.D. thesis, U. of Ottawa, 1978.

He 51 N.F.M. Henry et al, The interpretation of X-ray diffraction photographs, Macmillan & Co, London, 1951.

Is 74 J. Isomura, F.G.D. Prat and J.C. Woolley, Phys. stat. sol.(b), 65, 213 (1974).

La 66#1 G.R. Lachance and R.J. Traill, Canadian Spectroscopy, 11, 43 (1966).

La 66#2 G.R. Lachance and R.J. Traill, Canadian Spectroscopy, 11, 63 (1966).

La 70 G.R. Lachance, Canadian Spectroscopy, 15, 64 (1970).

Ma 72 Denis Martel, M.Sc. thesis, U. of Ottawa, 1972.

Mu 72 Rudolf O. Muller, Spectrochemical analysis by X-ray fluorescence, Plenum Press, ew York, 1972.

Sm 59 R.A. Smith, Semiconductors, University press, Cambridge, 1959.

Th 67 Alan G. Thompson and J.C. Woolley, Can. J. Phys., 45, 255(1967).

Th 69 M.B. Thomas, Ph.D. thesis, U. of Ottawa, 1969.

We 70 R.W. West,ed., Handbook of Chemistry and Physics, The Chemical Rubber Co., Cleveland, 1970.

Wi 62 R.K. Willardson and H.L. Goering, eds., Compound Semiconductors, Vol. 1, Ch. 1 (J.C. Woolley), Reinhold Pub. Co., New York, 1962.

Wi 66 R.K. Willardson and Albert C. Beer,eds., Semiconductors and Semimetals Vol. 3, Ch. 6, , Academic Press, New York, 1966.

Wi 72 R.K. Willardson and Albert C. Beer,eds., Semiconductors and Semimetals Vol. 8, Ch. 6, , Academic Press, New York, 1972.

Wi 78 C.K. Williams et al, Journal of electronic materials, 7, 639 (1978).